HHS Public Access

Author manuscript

Chem Soc Rev. Author manuscript; available in PMC 2016 May 03.

Published in final edited form as:

Chem Soc Rev. 2016 March 29; 45(7): 1958–1979. doi:10.1039/c5cs00581g.

Clinical instrumentation and applications of Raman spectroscopy

Isaac Pence and **Anita Mahadevan-Jansen**

Department of Biomedical Engineering, Vanderbilt University, Nashville, Tennessee, USA

Anita Mahadevan-Jansen: Anita.Mahadevan-Jansen@Vanderbilt.edu

Abstract

Clinical diagnostic devices provide new sources of information that give insight about the state of health which can then be used to manage patient care. These tools can be as simple as an otoscope to better visualize the ear canal or as complex as a wireless capsule endoscope to monitor the gastrointestinal tract. It is with tools such as these that medical practitioners can determine when a patient is healthy and to make an appropriate diagnosis when he/she is not. The goal of diagnostic medicine then is to efficiently determine the presence and cause of disease in order to provide the most appropriate intervention. The earliest form of medical diagnostics relied on the eye – direct visual observation of the interaction of light with the sample. This technique was espoused by Hippocrates in his 5th century BCE work *Epidemics*, in which the pallor of a patient's skin and the coloring of the bodily fluids could be indicative of health. In the last hundred years, medical diagnosis has moved from relying on visual inspection to relying on numerous technological tools that are based on various types of interaction of the sample with different types of energy – light, ultrasound, radio waves, X-rays *etc.* Modern advances in science and technology have depended on enhancing technologies for the detection of these interactions for improved visualization of human health. Optical methods have been focused on providing this information in the micron to millimeter scale while ultrasound, X-ray, and radio waves have been key in aiding in the millimeter to centimeter scale. While a few optical technologies have achieved the status of medical instruments, many remain in the research and development phase despite persistent efforts by many researchers in the translation of these methods for clinical care. Of these, Raman spectroscopy has been described as a sensitive method that can provide biochemical information about tissue state while maintaining the capability of delivering this information in real-time, non-invasively, and in an automated manner. This review presents the various instrumentation considerations relevant to the clinical implementation of Raman spectroscopy and reviews a subset of interesting applications that have successfully demonstrated the efficacy of this technique for clinical diagnostics and monitoring in large ($n \geq 50$) *in vivo* human studies.

1. Why Raman spectroscopy?

As described by Dr C. V. Raman in 1928, the Raman signal is usually weak (one in one hundred million incident photons) and "requires very powerful illumination for its observation."[1] Today, advances in laser sources and sensitive detectors enable the

Correspondence to: Anita Mahadevan-Jansen, Anita.Mahadevan-Jansen@Vanderbilt.edu.

application of this scattering event for samples that are more complex than the original "dust-free liquids or gases." Raman peaks are typically spectrally narrow (a few wavenumbers) and in many cases can be associated with the vibration of a particular chemical bond (or normal mode dominated by the vibration of a single functional group) within a molecule.[2] Fig. 1 displays an example Raman spectrum, that of phosphatidyl-choline, a phospholipid molecule, where each band can be correlated to specific stretching and bending modes of vibration in the molecule, thus providing a molecular fingerprint. Consequently, in tissue, which is composed of a complex mixture of molecules, the presence of the unique bands of phosphatidyl-choline can be tracked resulting in the quantitative evaluation of the sample's chemical composition. Such quantitative or qualitative assessment in turn can be used to infer specific biochemical changes associated with tissue pathology or physiology for diagnosis or monitoring.

Thus Raman spectroscopy is a molecular specific technique that can be used to develop a fundamental biochemical understanding of tissue physiology and pathology and extend this knowledge for tissue diagnosis and monitoring. The optical nature of the technique makes it possible to extract this information non-invasively, or at the very least non-intrusively, facilitating the utility of this technique in a clinical setting. Because Raman scattering is both a sensitive and weak phenomenon, instrument considerations for adapting this technique for clinical applications can be challenging. Since the initial reports of *in vivo* human tissue spectra in 1993,[3] technological development and technique refinement have enabled Raman measurements in humans with integration times of 0.5–5 seconds allowing real-time assessment of tissue state.[4–6] Spectra can now be collected, corrected for undesirable signal components, processed and analyzed rapidly to provide automated feedback at the time of measurement.[7–9] With these advancements, Raman techniques satisfy many of the criteria required for the adoption of a novel biomedical diagnostic technique in clinical practice: sensitivity to changes in tissue, *in vivo* application, and unique information obtained noninvasively, in real time.[10] This review will focus on the considerations vital to efficiently implementing Raman spectroscopy for *in vivo* clinical applications in diagnosis and sensing and some of the major clinical research under continued investigation.

2. Clinical instrumentation

A dispersive Raman system is similar to most optical spectroscopic systems and consists of three primary components – light source, sample light delivery and collection, and dispersive element with detector (Fig. 2). The specifics of these components are challenged by the needs of the clinical setting and application. Like standard medical instruments, a clinical Raman system should be small and easily transportable, optical alignment and calibration should be robust, sample light delivery and collection should be sterilizable and rugged, and the detection system should be sensitive to the weak biological signals.

The components that comprise a clinical Raman system can be broadly categorized into excitation and detection branches. Excitation is achieved by delivering the light from a given laser source to the tissue site of interest, in general by means of a fiber-optic probe or an articulated light delivery arm. The Raman scattered light is then collected, often through the same delivery system, and directed to a spectrograph and detector. As the technology

utilized *in vivo* for clinical measurements has developed, so too has the breadth of individual components that have been investigated and accepted within these systems. The following sections will discuss many of the requirements for the individual components in order to perform clinical Raman spectroscopy.

a. Lasers

Due to the weak nature of Raman scattering, it is imperative to deliver sufficient power to the sample in order to generate Raman scattered photons for detection in a reasonable integration time relevant to the clinical setting under consideration. However, Raman scattering is mediated by the other competing optical phenomena within the sample. Furthermore, it is important to consider issues such as maximum permissible exposure (determined by ANSI or similar organizations)[11] and temperature increase (relevant to patient comfort and minimizing tissue damage).[12] Laser power then becomes a function of identifying a compromise between signal to noise, patient safety and comfort, and instrumentation considerations. Choice of laser is also governed by other factors such as laser stability especially when using a multimode laser. Raman lines are narrow and highly specific for a given vibrational mode. This then implies that the precise position and width of the Raman line requires the excitation source to be stable in wavelength position, bandwidth, and spatial mode for consistent results. Having accounted for these factors, the properties of the target tissue or sample are one of the major criteria for the choice of laser excitation source for a clinical Raman instrument. Since Raman shifts are relative to the Rayleigh (excitation) line, similar results can theoretically be obtained from many different instrument configurations. However, the optical properties of the samples, including scattering and total attenuation coefficients as well as excitation, emission, and yield properties for any endogenous fluorophores present in the sample, are critical factors for consideration. The impact of each of these parameters is a function of wavelength.[13] Samples with high attenuation coefficients will limit the ability to deliver and collect the light beyond very superficial layers. Furthermore, strong absorbing molecules in a sample can also lead to the generation of excess heat deposition in the tissue, which can cause damage with high irradiance. Likewise, the presence of strong fluorophores can generate signals that overwhelm the modest Raman peaks that are concurrently detected. Due to the associated decrease in total attenuation coefficient for the major absorbing molecules in many biological tissues (water, melanin, oxy- and deoxy-hemoglobin), NIR excitation sources are commonly chosen for clinical instruments.[14] Further, since few known biological fluorophores have their peak emission in this region of the spectrum, with a noted exception of melanin, moving to the NIR wavelengths for excitation results in lower fluorescence background in the tissue at these wavelengths and simplifies the signal processing needed for extracting the Raman bands compared with visible or UV excitation.[15] As depicted in Fig. 3, tissues such as the breast (A) that do not have strong autofluorescence signals relative to the Raman features can be collected with several different wavelengths; however, highly autofluorescent tissues like the kidney (B) require the use of longer excitation wavelengths to obtain useful Raman spectra. Thus tissue properties are vital considerations when choosing the laser source for the clinical application of Raman spectroscopy.

Early Raman systems were based on the argon ion laser for visible excitation,[16,17] Nd:YAG (neodymium doped yttrium aluminum garnet) laser for FT-Raman applications,[18] and titanium:sapphire (Ti:Sapph) laser for NIR excitation. High output powers, single spatial and longitudinal modes of operation, and Gaussian beam profiles enable near-diffraction-limited optical performance for all of these sources.[19] However, the size of these lasers and their electronic and cooling requirements limit their practicality in a portable clinical Raman system. Some current Raman instruments, especially those with confocal capabilities, still use the Ti:Sapph laser. The development and continued advancement of diode laser technology has completely changed the footprint of a typical Raman system. Diode lasers utilize electro-optical components (diodes), which emit light as a function of both applied current and operating temperature.[20] Diodes themselves are small (<1 mm^3) and require highly accurate controlling electronics to obtain the stable output necessary for Raman excitation. Without highly stabilized thermal and current control, laser diodes are prone to thermo-elastic effects on the laser cavity length (and thus output frequency) and output power fluctuations, respectively. Laser diodes are also characterized by their elliptical beam output (rectangular shape of the output facet) and astigmatism (unequal beam divergence from each dimension of the rectangular facet). These factors complicate free beam coupling of diode lasers, typically requiring beam shaping optics for successful implementation. Most commercial diode lasers are available with a pigtail option to directly couple a fiber to the laser diode to minimize the losses due to astigmatism and elliptical nature of the beam.

More recently, external cavity diode lasers (ECDLs) have emerged as robust and cost-effective light sources for Raman applications. The extended length of the resonant cavity of the laser diode minimizes the effect of small thermo-elastic changes on the output frequency by extending the distance between the diode's longitudinal modes. Compared with a standard laser diode, the ECDL diminishes mode hops, minimizes the spectral bandwidth of output light, permits wavelength tunability, and decreases temperature-dependent frequency response.[21] The laser linewidth of <0.001 nm (at 785 nm) with mode locking provided by an ECDL is vital for medical applications where measurement repeatability and spectral resolution are important performance parameters. ECDLs are commercially available in tunable Littman–Metcalf or Littrow configurations, and can be made at specific wavelengths using distributed Bragg reflector configurations.[22,23] Mode stabilized diode lasers with powers on the order of 300 mW, either in single mode or multimode configurations, designed specifically for Raman spectroscopy are commercially available, lightening the burden for those developing clinical Raman systems.

b. Fiber optic probes

Clinical application of Raman spectroscopy requires the delivery and collection of light to and from the sample (tissue). This is typically mediated through the use of optical fibers configured to maximize signal collection while minimizing interfering signals generated in the fibers and related optics themselves.[24] Since fiber optic probes will be discussed in a related manuscript in this special issue, here we only present considerations relevant to clinical translation. Depending upon the constraints of the clinical target, probe designs can be tailored to best interface with a sample and access the region of interest. Design considerations are dependent on the Raman configuration under study (discussed later),

location of organ under study, micro-anatomy of the tissue, and pathophysiology of the disease.

A critical aspect for consideration in translating Raman spectroscopy from the laboratory to the clinic is the inherent nature of Raman scattering. Raman scattering is a weak phenomenon but most materials are Raman active, and therefore the materials used in the Raman system generate Raman signals that interfere with the detection of sample signal.[25] Most fiber optic probes use optical fibers made of low-OH silica which has been extensively used in many applications of light in a clinical setting.[26] Silica is inherently inert, amenable to sterilization, and relatively low-cost, making it the material of first choice when designing fiber probes. Unfortunately, silica has a strong Raman signal, with several bands that can overwhelm sample signal.[25] This fiber signal can have magnitudes equal to and sometimes greater than that of the sample under study and thus any probe design needs to account for this behavior.[27] Fiber signal can be generated in the delivery fiber core and cladding by the excitation light. In addition, background signal can also be generated in the collection fibers by any excitation wavelength light returning into the collection fiber(s).[27,28] Mathematical techniques typically fail to de-convolve this unwanted fiber signal from sample signal as silica signal strength depends on the reflective and scattering nature of the sample and photon loss due to fiber bending. A feasible probe design that uses silica fibers must therefore prevent silica signal generated in the delivery fiber from illuminating the sample as well as prevent elastically scattered excitation light from entering the collection fibers and generating this signal.

Several different designs have been proposed for potential clinical acquisition of Raman spectra using silica based fiber-optic probes.[25,29] Since the earliest design reports, most fiber designs have been based on similar concepts with modifications. In general, Raman probe designs utilize a band-pass filter placed after the excitation fiber lens, thus allowing only transmission of the excitation light. To achieve this, dielectric bandpass filters have been used to blue shift the wavelength cutoff with increasing angle of incidence and have therefore been shown to act as a one-way mirror for elastically scattered light.[30] This phenomenon increases the overall efficiency of the probe by preventing multiple scattered incident photons from exiting the tissue and returning into the source fiber. Longpass or notch filters are placed in front of the collection fibers to block the transmission of Fresnel reflected excitation light as well as to prevent the elastically scattered light from entering the collection fibers. These filters can be placed either at the tip of the probe, at fiber connections within the probe, or deposited directly on the end of the fibers themselves to maximize effectiveness, generally requiring sizes on the order of a few millimeters or smaller for distal tip filtering. There is thus a demand for high-quality optical coatings and micro-optical components that will simplify the design of much needed compact fiber-optic probes for Raman spectroscopy in biomedicine. Alternatively, non-silica based materials such as crystalline fibers and hollow waveguides have been evaluated for Raman applications;[31,32] however, these have not been tested for clinical use and as such are not included here.

The different silica fiber based probe designs available commercially yield different sample geometries and probe diameters, which in turn affect the application under consideration. It

is therefore critical to consider the anatomy of the sample to be studied along with the pathophysiology of the disease to be measured so that appropriate sampling may be achieved.[33] For example, when studying the inner lining of the colon, where the epithelial lining has a variable layer thickness based on disease status, it is important that the probe be designed to sample only the superficial layers of the tissue and not into the deeper tissue.[34] A number of different sampling probes have been developed in order to meet specific design criteria, such as rapid acquisition time, depth selectivity, or the collection of data sets from complementary modalities.[35–39] Some of the most common probe designs and associated vendors are listed in Table 1.

c. Spectrographs and detectors

A typical dispersive Raman detection system used for potential clinical applications consists of a short focal length imaging spectrograph attached to a cooled charge-coupled device (CCD) camera. Clinical implementation of Raman spectroscopy requires spectral acquisition of no more than a few seconds. This fast acquisition in turn needs a fast spectrograph and a highly sensitive detector, particularly given the weak nature of the Raman signal. A typical CCD camera used in spectroscopy consists of a rectangular chip wherein the horizontal axis corresponds to the wavelength/wavenumber axis and the vertical axis is used to stack multiple fibers for increased throughput, which can subsequently be binned for improved signal to noise ratio (SNR). Technological advances have led to CCD chips with quantum efficiencies on the order of 90% in the NIR (this information can be found on any of the CCD vendors' (Table 1) websites). While different types of chips are commercially available for different applications, a back-illuminated, deep-depletion CCD is highly recommended for NIR Raman spectroscopy. These chips are however known to be susceptible to the so-called etaloning effect,[40–42] wherein the thin silicon chip acts as an etalon resulting in the introduction of sharp peaks in the sample signal that are hard to resolve from the narrowband Raman signal. However, CCD cameras are now available commercially that effectively eliminate this effect.[40–42] Most CCDs in Raman use a thermoelectric (TE) multistage Peltier system to actively cool the camera down to at least −70 °C in order to realize excellent dark noise performance. In fact, current Raman systems for most biomedical applications are only limited by shot noise.

Tissue background signal is the bane of dispersive Raman spectroscopy, swamping the detector and hindering evaluation of sample Raman spectra. This background, especially in complex tissue samples, can arise from both the broadband emission of autofluorescence and elastic scattering of both stray excitation light and the Raman bands themselves. Non-collimated light and angular dependent filter performance can add substantial background to a spectrum, as can the scattering and spectral broadening of Raman peaks themselves; these phenomena are continuously variable with wavelength.[43] The presence of fluorophores in samples also contribute broad background signal to the collected Raman spectrum and are mediated by the wavelength dependent excitation for the comprising chromophores. However, most tissue fluorophores, with the exception of porphyrins and melanin,[44] have their excitation and emission maxima at UV and visible (UV/VIS) wavelengths.[45] Therefore, longer visible and NIR sources at wavelengths such as 633, 785, and 830 nm are preferred over those in the UV/VIS to reduce the amount of both fluorescence interfering

with the detectable Raman signal. Selection of appropriate NIR wavelengths for excitation is often governed by competing factors. The longer the wavelength, the lower is the fluorescence and scattering background to be rejected; however, the Raman scattering also decreases. Again as demonstrated in Fig. 3, where 785 nm excitation was plagued by autofluorescence and scattering in kidney tissue (B) that was mitigated by 1064 nm excitation. Further, while silicon CCD detectors are capable of excellent performance over most of the NIR, the quantum efficiency decreases rapidly with wavelength, falling to below 15% at 1000 nm. Therefore, competing parameters of Raman scattering intensity, tissue background, and detector efficiency need to be assessed relative to the tissue under study to determine the wavelength range to be used. Overall, researchers in this field tend to prefer 785 nm excitation as a reasonable compromise for most tissues (as surveyed from the publications reviewed in Table 2). It should be noted that when acquiring Raman spectra in the high-wavenumber region (2400–3800 cm^{-1} in tissues) which is about 967–1118 nm for 785 nm excitation, obtaining high SNR Raman signals can be difficult using silicon-based detectors due to the decreasing quantum efficiencies. For detection of wavelengths above 950 nm, other types of detectors such as indium gallium arsenide (InGaAs), germanium, and indium phosphide (InP) detectors need to be used. However, these detectors suffer from lower quantum efficiency and increased noise in comparison to silicon detectors.[46] Nevertheless, instrument configurations utilizing Nd:YAG sources and multichannel InP/InGaAsP detectors have recently reported the feasibility of Raman spectroscopy in tissues such as the lung and gastric tissue at 1064 nm excitation with acquisition times on the order of hundreds of seconds.[47,48] *Ex vivo* reports by the authors have also recently demonstrated the potential for clinically relevant applications of dispersive 1064 nm Raman instruments, particularly for in tissue type with a high fluorescence background at 785 nm (Fig. 3).[12,49]

A Raman-sensitive detection system capable of clinical measurements requires an appropriate imaging spectrograph that couples to the sample interface (such as a fiber probe) on one end and the CCD of choice at the other end. Compact, rugged, spectrographs optimized for Raman use are now commercially available with f-number matching to the numerical aperture (NA) of optical fibers and high throughput for rapid acquisition (see Table 1). In order to resolve details of the biological Raman bands, the Raman detection system should have a spectral resolution of at most 8 cm^{-1}. Since spectral resolution depends on coupling optics, slit size (or fiber size if no slit is used), and CCD pixel size, each of these plays a crucial role in the design and selection of the detection system.[50] It is common to use 200–400 micron core diameter fibers in the fiber optic probe for maximum signal collection at the sample. However, this stack of fibers placed at the entrance port of the spectrograph will significantly reduce the spectral resolution of the system. If one assumes 1 : 1 matching of fiber-spectrograph optics, 200 μm core collection fibers stacked at the entrance port of the spectrograph, no slit (or a 200 μm slit) and 25 × 25 μm CCD pixel size, the resulting spectral resolution is 15.14 cm^{-1} for a 6.13 nm mm^{-1} dispersion grating (typical for holographic gratings).[51] One can reduce the entrance slit to 100 μm and/or reduce the collection fibers used to 100 μm core diameter and achieve a spectral resolution of 7.6 cm^{-1} which is close to what is needed to resolve tissue Raman peaks. Since the beams out of the fibers are Gaussian, one can speculate that when using a smaller slit size with larger fibers, the loss of Raman photons is not as significant since one is only cutting out the

tail of the beam. Further, larger fibers are easier to work with when building a filtered probe than smaller diameter fibers. Thus making these spectral calculations when designing the Raman system, particularly with respect to dispersion and therefore spectral resolution, needs to be tracked during the selection of each of the components needed for the Raman detection system.

Additional components of the detection system include rejection filters that remove any laser light as well as the elastically scattered light from the detected signal. Holographic notch filters can block the laser wavelength with an optical density of six with steep edges and provide 90% transmission elsewhere with a relatively flat curve.[52] For dispersion, holographic transmissive gratings generally have the highest throughput performance,[53] however, most of these are implemented in fixed positions, enabling measurement of only part of the Raman spectrum at a time. Furthermore, the performance of these components can drift over long periods of time (years), potentially due to environmental degradation (humidity, temperature). There has recently been renewed interest in reflective and prism-based approaches to dispersion.[54,55] Reflective gratings can usually cover a larger range of the spectrum at high spectral resolution, but often result in a longer integration time due to lower efficiency and movement of the grating position. Some devices circumvent this issue by including versatile options for either static or full-range spectral measurements, or include gratings with different dispersion elements to achieve high resolution. In general, instruments with multiple gratings also have a larger footprint than those with fixed gratings. Size is an important consideration when designing a clinical device as the space available in most clinical procedure rooms is at a premium. The needed small footprint is also directly at odds with spectrograph designs that reduce performance-limiting aberrations based on long focal lengths. Some groups have attempted to account for field curvature distortions in transmissive systems by carefully designing the detector end of the fiber probe to have a parabolic shape that will appropriately map to a vertical line on the detector, limiting signal overlap and improving spectral resolution.[56] Newer instrument designs have been implemented using corrective optics or beam shaping techniques to reduce the impact of aberrations, however, these instruments have yet to be reported for clinical investigation. Another technique available for use in the bench-top setting is hyperspectral Raman imaging, collecting high resolution global mapping *via* monochromatic images.[57] This snapshot technique provides spatial information for samples rapidly however has not been implemented in clinical investigation to this point. Increased research studying the high-wavenumber band has also resulted in the commercial availability of spectrometers with extended spectral coverage at the expense of either resolution, integration time or overall size. However it should be noted that several spectrographs that meet the needs of a portable Raman system are available; these spectrographs are compact in design and rugged for portable use (see Table 1).

Most Raman measurements in medical applications today rely on state-of-the-art, high-cost, high-performance Raman systems that are compact and highly sensitive to the weak biological Raman signals.[58,59] While each researcher has his or her preferences on the specifics of the different components in the system, the design is ultimately driven by the tissue/organ under study and the pathophysiology of the process to be monitored. Table 1

presents the most common lasers, fiber probes, spectrographs and CCD cameras used to build clinical Raman systems as described in the papers listed in Table 2.

In describing and guiding the selection of each of the components described above, it is presumed that Raman spectroscopy is the only modality under consideration, and the Raman configuration to be used is dispersive Raman spectroscopy, to assess biochemical signatures associated with the biomedical problem under study in the fingerprint or high wavenumber region. These components can be obtained from any number of vendors or developed within a laboratory to assemble a system suitable for the specific study under consideration. It is vital for any clinical application that the individual components integrate into the most efficient instrument configuration possible and all spurious sources of confounding signals be minimized through design.

d. Data processing and analysis

i. Instrument calibration—Based on the previous section, it becomes readily apparent that to compare Raman spectra acquired from different tissues requires some standardized methods of calibration and processing that enable transferability of these spectra. Fig. 4 presents a flowchart of the major procedural steps and their order for converting raw measurement data from the detector to signals ready for comparison and analysis. Source compensation is a standard process that can be applied to control for variability in the source from measurement to measurement. This step is critical only when absolute intensities are necessary for analysis. Instrument response variations require two types of calibration: spectral calibration and intensity calibration. Spectral calibration is used to convert the horizontal axis from CCD pixel number to relative wavenumber. The emission spectrum of a known calibrated light source, such as a neon lamp with numerous and narrow bands in the NIR, is typically used to calibrate the horizontal axis into absolute wavenumbers (cm^{-1}). Relative wavenumber calibration is performed using the spectral position of the laser line and then validated using standards with well characterized Raman features and strong Raman scatter, such as naphthalene and acetaminophen. Spectral standards such as the fluorophore rhodamine 6G and a weak Raman scatterer such as methylene blue or vitamin E can be used as additional intensity standards to account for day-to-day variations in the spectral intensity.[60] Calibration of the intensity axis (spectral response correction) is necessary to account for the wavelength-dependent response of the various components in the detection leg of the system including the grating, the filters, optics as well as the quantum efficiency of the CCD chip. This is typically performed using a calibrated source such as a tungsten lamp certified by the National Institute of Standards and Testing (NIST) to generate intensity correction factors for variations in instrument throughput.[61] This calibration process is essential for comparison of spectra measured across different Raman instruments for the same or similar sample. This calibration is typically performed early in a study and then on a regular basis to validate the accuracy of the correction factors over time. However, perturbation of any of the optical components including those induced by moving the system from the laboratory to the clinic can affect the calibration and therefore an additional method that accounts for day-to-day calibration of the system performance must also be developed. Collection of a NIST lamp intensity spectrum is often impractical in a clinical situation due to the experimental controls necessary to ensure that the bright, diffuse

emission of the lamp traverses only its intended path through the Raman instrument to the detector, along with the safety concerns that correspond to the spectral intensity in the UV portion of the spectrum. More recently, spectral intensity standards consisting of green-colored Schott glass have been explored by NIST[62] and other groups[63] as more practical alternatives for daily calibration, but no consensus has yet to be reached on their applicability as a Raman standard.

As indicated in Table 1, it is possible to configure a Raman system using different combinations of a laser, spectrograph, probe and detector. In a parametric study of laser, probe, and CCD detector combinations for a single spectrograph, the influence of each component in an instrument configuration on reliability and reproducibility of Raman spectra was investigated (unpublished). The various combinations of these components can be seen in Fig. 5. By isolating the impact of each instrument, this work identified that the most significant impact on the obtained signal was driven by the fiber optic probe. When a single probe was maintained across different lasers, spectrographs, and CCDs, the total variance of the detected signals decreased significantly relative to signals obtained when spectra were combined across probes. This data highlights the importance of using a single probe design for data collection for a given clinical application.

Even when a single probe design is selected for a given clinical Raman instrument, it is important to precisely account for instrument-induced variability. The aforementioned variability study indicates the importance of using a single probe design for clinical data collection (Fig. 6A). However, it is not feasible to conduct a large clinical study or manufacture a potential medical device that relies on a single probe for the lifetime of the instrument. As multiple probes built from a single design are used, it should be noted that each optical component can have a similar but ultimately unique wavelength-dependent response. As depicted in Fig. 6 for different *in vivo* tissue measurements with unique probes of the same design, differences in filtering and throughput can impact not only raw signals (Fig. 6B) but also impact the resulting, processed spectra (Fig. 6B, inset). However, current calibration methods do not provide adequate calibration to minimize probe response which in turn affects data analysis when spectra across multiple probes are combined.[60] Practically, this data indicates the necessity of adequately calibrating probe-specific signals thoroughly for successful implementation of Raman techniques and the community needs to work together to develop such methods. In the meantime, it is recommended that investigators acquire multiple probes based from a single design and built at the same time, to minimize this variability.

ii. Data processing

1. Fluorescence & background elimination: The increased investigation of Raman spectroscopy for biological and clinical purposes is largely due to its high sensitivity to subtle biochemical changes and its capability for nonintrusive application. One challenge faced in these investigations is that biological applications involve turbid, chemically complex, and widely varying targets. Therefore, significant challenges exist for both acquiring viable Raman signatures and suppressing the noise sources inherent to the target medium. The greatest challenge for obtaining Raman spectra from biological materials is the

intrinsic fluorescence and elastic scattering of many organic molecules. Often several orders of magnitude more intense than the modest Raman signals, this background, if left untreated, will likely dominate the Raman spectrum and hinder analysis and interpretation of tissue biochemistry. To extract Raman signal from the raw spectra acquired, elimination of fluorescence signal is necessary. While most biological fluorescence occurs in the UV/VIS and intensity decreases as a function of wavelength, the fluorescence and scattering background observed for NIR still interferes with the measured Raman spectrum (Fig. 3B). The intensity of this background is generally dependent upon tissue but is ubiquitously present in almost all tissues studied, meriting attention prior to spectral analysis.

Both hardware and software techniques have been proposed for background subtraction from raw Raman signals. Wavelength shifting and time gating are hardware-based techniques that have been shown to effectively minimize fluorescence interference in Raman spectra but require specific design considerations for the spectroscopic system to achieve their results.[64,65] Several software-based mathematical methods can be implemented without system modification and are generally preferred for fluorescence removal. Such techniques have included first- and second-order differentiation,[66,67] frequency domain filtering,[64] wavelet transformation,[68,69] multistage smoothing,[70] and polynomial fitting.[7,71,72] Each of these methods has been shown to be useful in certain situations, however all have their advantages and limitations that must be evaluated before selecting a method for application with a given system.

First and second order differentiation relies on invariant wavelength-dependent fluorescence emission compared with the relative shifts measured in Raman spectra. One way to accomplish this differentiation is by measuring the spectra at two (or more) slightly shifted excitation wavelengths (within a few nanometers) and taking their difference.[73] Integrating the difference spectrum results in the original Raman signal. Similar results can be achieved with a single excitation wavelength by taking the first derivative of the spectrum and integrating the noise-smoothed derivative spectrum following baseline correction.[64,67] The derivative method for fluorescence subtraction is efficient and unbiased, but distorts Raman line-shapes and relies on complex mathematical fitting algorithms to reproduce a traditional spectral form.[64] While many of these methods were developed and tested in the early 1990s, shifted excitation methods for removing this undesirable fluorescent signal, coined as modulated wavelength Raman spectroscopy, are coming back into vogue, utilizing multiple closely spaced excitation sources and signal processing algorithms to remove fluorescence signal.[74] Newer sources allow the use of multiple excitation wavelengths to improve the accuracy of the method; however, removal of the DC offset remains an issue.

Frequency filtering and polynomial fitting are other common methods for fluorescence elimination. Frequency filtering can be achieved with fast Fourier transform (FFT), transforming the spectrum to the frequency domain by taking the FFT which is then be multiplied with a linear digital filter to eliminate the fluorescence. The inverse FFT yields the Raman spectrum free of fluorescence.[64] If the frequency elements of the Raman and noise features are not well separated, this method can generate artifacts in the processed spectra. A more direct method to subtract fluorescence that is both simple and accurate is to fit the measured spectrum containing both Raman and fluorescence information to a

polynomial of sufficient order to describe the fluorescence lineshape without capitulating the higher-frequency Raman lineshape.[7] Polynomial curve fitting has an advantage over other fluorescence reduction techniques due to its inherent ability to retain the spectral contours and intensities of the input Raman spectra and can be easily implemented in MATLAB® or other computing platforms for automated performance.

Individual techniques have advantages and disadvantages; the method used should be selected based on the specific application and best matched to measurement technique. Mosier-Boss *et al.* tested the use of the shifted excitation, first derivative, and FFT techniques for fluorescence subtraction and indicated a preference for using the FFT based on its ability to filter random noise from the spectrum.[64] In an analysis of the different techniques by the author for *in vivo* tissue applications, the use of a polynomial fit was found to be the optimal technique for both experimental and computational considerations. More recently, a modified polynomial fitting algorithm that accounts for noise levels has been proposed[72,75] which has been shown to minimize the presence of artificial peaks in low SNR spectra that are common in measurements of tissues with high autofluorescence. It should be noted that order of the polynomial used is specific to the sample fluorescence lineshape and as such should be determined before utilizing this technique (Fig. 7).

Other methods have utilized advanced signal processing techniques to separate underlying autofluorescence from the desired Raman signals. Wavelet decomposition, penalized least-squares fitting techniques[76] and principal component analysis (PCA) have been described for suppression of the confounding signal components.[77] Wavelet transformation is dependent on the decomposition method used and the shape of the fluorescence background, whereas PCA assumes that the highest signal variance is due to the fluorescence background, which may be invalid for some applications. Thus, there are tradeoffs for each method and the choice may be governed both by the application at hand and the preference of the investigator.

2. Noise smoothing and binning: Since Raman scattering is such a weak phenomenon, the SNR of most measured Raman spectra requires significant noise smoothing in order to extract the underlying Raman bands. Various types of noise smoothing filters have been effectively used. These include the median filter, the moving average window filter, the Gaussian filter whose full width at half maximum is typically set equal to half the spectral resolution of the system, and the Savitzky–Golay filter of various orders.[59,78–81] Other methods include using PCA, genetic algorithms, and other multivariate statistical approaches to remove the higher order components and effectively removing noise.[82,83] In using any of these or other methods of noise smoothing, care should be taken to retain the integrity of the spectral lineshape especially when dealing with samples with multiple peaks that are close to each other. Validating the method using spectra from weak Raman samples (with low SNR) should be an essential step in the development process.

Other preprocessing methods typically applied include binning of the spectral data set due to the large number of variables (which is dependent of CCD chip size) for computational ease. Depending on the variability in the acquired data and the needs of the analysis methods used, various normalization methods may also be applied to allow comparison of the spectra.

Normalization methods include normalization to intensity standards, normalization to a spectrum's own maximum intensity or area under the curve, and mean scaling to the average spectrum acquired from a given patient. Some researchers prefer to use difference spectra to achieve the same normalization effect to account for intra- and interpatient variability observed.

iii. Data analysis—One of the advantages of spectroscopic diagnosis is automation, which allows objective and real-time diagnosis of pathologies. Spectral differences observed as a function of tissue physiology or pathology can be incorporated into diagnostic algorithms that can in turn be implemented in real-time to yield classification using univariate and multivariate statistical methods; several statistical approaches have been identified and applied for feature extraction and classification of tissues towards automated, clinical diagnosis. Since Raman spectroscopy is a biochemically specific technique, chromophore and scattering molecule contributions can be extracted from the measured spectra. These can then be used in diagnostic algorithms as well as in understanding of the spectral signature as it pertains to the disease process. For example, the extracted contributions can be used to quantify blood analytes for applications such as glucose sensing.[84]

Original analyses for Raman signals were based on differences in intensity, shape, and location of the various Raman bands between normal and abnormal cells and tissues. Observed differences between the different tissue types under study were selected for classification algorithms based on empirical methods using changes in intensity or ratios of intensities or number and location of peaks. For example, the intensity ratio of the CH_2 bending vibrational mode at 1440 cm^{-1} to the Amide I vibrational mode at 1655 cm^{-1} has been observed to vary with disease in several applications including breast cancers and gynecologic cancers and precancers.[85,86] The limitation to this approach however, is that diagnostically useful information may be contained in more than just the peaks or valleys observed in tissue; a method of analysis and classification that includes all the available spectral information may be important for the accuracy of detection. Further, empirical methods tend to be biased in favor of the spectral differences specific to the data set used for the analysis and these methods do not hold under validation. To obtain an unbiased estimate of the performance of algorithms for Raman data, multivariate statistical techniques have become the accepted practice for the development of discrimination and classification algorithms for diagnostic applications.

In the past few years, great strides have been made in the application of multivariate techniques for spectroscopic data analysis in disease detection.[61] Discrimination techniques such as linear and non-linear regression as well as classification techniques such as neural networks have been employed.[61,87] Data compression tools such as PCA are still commonly used to reduce the dimensionality of the data matrix and have been used to account for the variability in the data.[88] Linear and nonlinear methods have also been used for feature extraction. Subsequently, methods such as hierarchical cluster analysis (HCA)[89] and linear discriminant analysis (LDA)[87] have been used to yield classification algorithms for disease differentiation. Partial least squares, a regression-based technique, as well as hybrid linear analysis, have been used to model tissue based on component spectra, finding component contributions for disease detection and extracting accurate concentrations of analytes such as

glucose using NIR Raman spectra for transcutaneous blood analysis.[90,91] More complex multivariate and machine learning methods have also been utilized, including support vector machines,[92] logistic regression models,[49,93] genetic algorithms,[82] neural networks,[94] decision trees,[95] optimization techniques,[91] and generalized linear models. These methods allow the integration of non-Gaussian constraints and variable weights to optimize classification performance. However it should be noted that these complex methods may not necessarily provide a significant improvement in the diagnostic performance of Raman spectroscopy and as such most studies tend to rely on simpler (and often linear) albeit multivariate methods of discrimination.

In small sample sets, one often relies on the leave-one-out or K-fold methods of cross validation, as well as nested methods for multiple optimization steps. Rigorous, unbiased estimates may be obtained by developing robust discrimination algorithms using a test set and its performance quantified in a validation set. Ideally, these two sets are formed by random distribution of the subject population into two equal data sets. The true measure of success of Raman spectroscopy for tissue diagnosis requires validation of the tested algorithm in an extensive unbiased (and independent) validation set.[96]

Analyzing Raman signals for spectral differences and developing diagnostic algorithms for the purpose of disease classification are one facet of the clinical application of Raman spectroscopy for tissue diagnostics. However, the wealth of information provided in Raman spectra especially with respect to molecular composition enables identification of the nature and biochemical processes responsible for these changes. This information can be used to enhance fundamental understanding of various biological processes as well as inform the improvement of diagnostic performance.

Several researchers have harnessed the benefit of extracting physiologically relevant markers from Raman spectra of tissues. Puppels *et al.* obtained quantitative information about skin hydration based on Raman spectra.[97] Feld *et al.* developed comprehensive models for biochemical component extraction that were used for disease classification.[98] More recently, Huang *et al.* performed semi-quantitative biomolecular least-squares modeling based on representative basis spectra in order to distinguish spectral sources for neoplastic lesions in multiple patients.[99] Each of these methods is based on the acquisition of Raman spectra from individually identified chromophores either as morphological tissue components, as extracted biochemical constituents, or commercially available pure chemicals. Pixelated Raman microspectroscopy has been used (with or without confocality) to measure Raman spectra from individual morphologic tissue components using tissue sections. A Raman spectrometer is coupled to a microscope and is scanned across the tissue section to obtain Raman images that can then be correlated with serial hematoxylin- and eosin (H&E) stained sections to identify relevant morphologic components and their Raman signature. Alternatively, tissue scatterers can be extracted from biochemical assays and Raman spectra can be acquired from each of these extracted chromophores using the same instrument as used to measure the biological specimen. Using mathematical models such as those developed by the Feld group, contributions of each of the extracted or morphologic components can be calculated for the intact tissue.

Thus, a portable, clinically viable instrument with a fiber-optic probe can be used to acquire Raman spectra *in vivo*. The ability of Raman spectroscopy in a particular tissue can be tested in animals *in vivo* or *in vitro* and subsequently applied for *in vivo* human detection. The acquired spectra can then be processed and analyzed and information extracted about the performance of the technique as well as about the biochemical components that contribute to the signals obtained by the method.

iv. Technology interface, control, and automation—A major feature that is paramount for translation of Raman spectroscopy or any other laboratory technology to a medical clinic is the constraint of an intuitive, automated interface. Given the inherent weakness of Raman scattering and the complexity of the generated signals, great care and effort must be spent in developing the instrument interface prior to deployment for a medical application. Thankfully, the instrument components discussed above can be combined in a manner appropriate for a detection target so that signals can be detected quickly. Once detected, the speed of modern computing technology can be utilized for real-time processing for background removal, component extraction, and class prediction. Optimizing algorithms for each step is vital for an intuitive interface along with practical considerations including how to best display feedback to the end-user. The first step towards successful integration is to implement a clinically-relevant user control. Hands-free enabled data collection with foot pedals or buttons at the probe interface are features that will enable clinical use, along with instruments that operate in real-time and provide continuous feedback. Zeng *et al.* and Huang *et al.* have reported systems that integrate data collection, processing, and analysis in times as low as 100 ms.[6,56,100,101] Even with the integration of rapid processing, the information provided by a complicated tool based on Raman spectra could be overwhelming. Combining this information into an easily interpreted display or audible feedback are vital steps for the clinical integration so that with minimal training, these devices can be deployed to benefit clinical medicine.

3. Raman configurations

Several different modalities of Raman scattering have been used to analyze the structure of various biological molecules.[102,103] Some of these techniques include ultraviolet (UV), visible or NIR dispersive Raman, Fourier transform Raman (FT-Raman), surface-enhanced Raman (SERS), and ultraviolet resonance Raman (UVRR) spectroscopy.[2,104] More recently developed techniques include stimulation Raman (SRS), tip-enhanced Raman (TERS), and coherent anti-Stokes Raman scattering (CARS).[105–107] Early adoption of Raman spectroscopy for biological applications with minimal interference from fluorescence relied on FT-Raman spectroscopy, where the Fourier transform of the scattered signal is detected, and subsequently inverse-transformed to give the actual Raman signature. This technique yields improved signal-to-noise ratio of hard to detect events but requires long collection times[97] that are not practical for clinical and *in vivo* implementation. With the recent developments in laser and detector technology, FT-Raman methods have become more or less obsolete at least as it pertains to clinical diagnosis and as such are not discussed here. Pursued extensively as a viable technique for *in vivo* human application, NIR dispersive Raman scattering is typically excited in the range of 780–1100 nm where minimal

fluorescence is produced making detection of the weak Raman signal easier, particularly in biological materials. However, several other configurations of Raman spectroscopy have been implemented *in vivo* and a summary of some of these as they pertain to potential clinical application are described below.

a. UV/VIS

While most implementations for clinical Raman spectroscopy rely on NIR excitation (785 or 830 nm), some researchers continue to use visible wavelengths for biomedical applications. The tradeoff between high Raman scattering cross-sections at lower excitation wavelengths and decreased penetration depth, higher absorption, autofluorescence, and heat generation usually limit the potential of *in vivo* clinical application with visible techniques. However, some studies continue to apply these more readily available excitation sources for various studies, particularly where direct interaction with the patient is not required.[108–110] Especially in applications of Raman spectroscopy for pathology analysis for which clinical protocols for *ex vivo* cytology and histology commonly employ conventional glass slides as the substrate, visible sources, such as 532 nm, demonstrate significant improvements in background signal relative to NIR excitation.[111] Other *ex vivo* work continues for several malignancies, including skin and oral neoplasia, with visible wavelengths that show promising results.[112–115]

Resonance Raman activation may be achieved when the excitation wavelength approaches electronic absorption of a molecule.[116] Resonance Raman excitation increases scattering signal intensity by several orders of magnitude. However, typical absorption frequencies of biological molecules such as proteins and nucleic acids occur at ultraviolet wavelengths where these wavelengths may cause photolysis of the sample and destroy it over time.[117] Further, the mutagenicity of UV radiation makes this technique inviable for clinical *in vivo* use.[118,119] As such, few researchers have pursued this approach for potential clinical applications in recent years.

b. Raman imaging

The weak nature of Raman scattering hinders the imaging of Raman features in biological materials such as cells and tissues with dispersive Raman spectroscopy in clinically feasible integration times. Intrinsic Raman imaging has been performed using the intensity of a specific Raman band or ratio of bands to build an image from cells and tissues.[120] As mentioned above, one method acquires a hyperspectral stack of monochromatic images over relatively large spatial areas. Another approach involves compiling a three dimensional data cube by measuring Raman spectra through point or line scanning of the excitation and collection beams.[121] The voxel size may be governed by the spatial resolution needed for the study and can be as small as the confocal pinhole up to ~100 s of micrometers. Both methods of imaging are performed on a Raman microscope and may require several minutes to hours to acquire an image depending on the spatial resolution thus making it infeasible for real-time clinical applications. Most studies with point or line scanned Raman imaging have been used to improve our understanding of biological processes in cells and tissues *in vitro* as well as in animal models.[19,122,123] Other methods of Raman imaging include nonlinear Raman techniques such as coherent anti-Stokes Raman spectroscopy (CARS) and stimulated

Raman scattering that take advantage of nonlinear processes for increased and selective signals. Both of nonlinear methods have been applied to study biochemical interactions in cells and tissues *in vitro* and *in vivo* applications have been confined to mouse models.[107,124–127] However, all these imaging techniques are restricted by the limited number of available Raman photons and therefore the long integration times necessary to acquire a Raman image successfully. As such none of these approaches have successfully been applied *in vivo* in humans and are not directly practical for clinical use.

c. Fingerprint *versus* high wavenumber

While the majority of researchers applying Raman spectroscopy for clinical applications have primarily been focused on spectral differences in the fingerprint range (up to about 1800 cm^{-1}), some studies have investigated the diagnostic utility of spectral features in the high-wavenumber, generally 2200–4500 cm^{-1} where distinct and strong features of lipids, proteins and water may be observed (Fig. 8). The fewer but broader features that occur in the high wavenumber region can be much higher in intensity relative to competing optical signals. Several studies have demonstrated the potential of high wavenumber Raman spectroscopy alone or in combination with fingerprint Raman methods to discriminate and classify disease *in vivo*.[128] Detecting high wavenumber Raman features pose different requirements on the Raman system design. Because the high wavenumber signal is inherently at a higher wavelength than the fingerprint, different gratings, filters and more importantly detectors may be necessary in order to efficiently collect signals especially when using common NIR Raman excitation sources (described in the detector section above). Alternatively, because the separation between the Rayleigh line and the detected Raman bands is so large, inline filtering can be mitigated, which has the potential to simplify probe designs and reduce cost, thus increasing the potential for clinical translation.

d. SORS

Perhaps the most impactful configuration of Raman spectroscopy in recent years has been the discovery of spatially offset Raman spectroscopy (SORS). Photon migration theory dictates that photons incident on the tissue surface that reemerge after only a few scattering events are likely to undergo minimal transverse shift and travel through the most superficial depths. Photons that undergo many scattering events are more likely to undergo a larger transverse shift and also travel deeper within the tissue, due to the fact that the scattering phase function of tissue is primarily in the forward direction. The combination of spatial offset with the Raman effect introduces depth selectivity in the spectral measurements expanding the ability of Raman spectroscopy to sub-surface phenomenon in biomedical applications.[129] The intensity of the Raman-scattered light at zero spatial offset includes contributions from both the superficial and underlying layers. However, as the spatial offset increases, the signal intensity from the superficial layers falls off more rapidly than the intensity of the signal from the underlying layers, which increases the relative proportion of signal from the deeper layers. The SORS signal can be collected through a range of spatial offsets, and computational techniques such as least-squares regression can be applied to separate the spectral signatures from individual layers.[130,131] It is important to note that while SORS can yield Raman spectra from deep within the tissue, it does so in a probabilistic fashion that relies on the layered architecture of tissues in which the spectral

signatures of the layers are distinct. This is in contrast to confocal Raman spectroscopy, which explicitly rejects out-of-focus light and collects spectra from a well-defined depth. This makes SORS better suited for low-resolution depth-dependent measurement of features and at greater depths (~centimeters) than confocal Raman spectroscopy (~100 s μm). Several researchers have applied SORS towards clinical applications in the bone and breast.[130,132,133] This approach has been extended to other configurations such as inverse SORS where the source and detection fibers are switched[134] and Raman tomography,[123] where SORS is combined with computed tomography and modeling of optical properties to obtain three dimensional Raman maps.

e. SERS

Surface enhanced Raman spectroscopy (SERS) is used to investigate the vibrational properties of single adsorbed molecules.[2,104,135] It was discovered that the rather weak Raman effect can be greatly strengthened (by a factor of up to 14 orders of magnitude) if single molecules are attached to metal nanoparticles of a suitable material and roughness to capitalize on both electromagnetic (surface plasmon resonance) and chemical enhancement.[136–138] Many groups have used SERS to detect single molecules attached to colloidal silver particles that are either adhered to a glass slide or in an aqueous solution. Single-molecule detection is of great practical interest in chemistry, biology, medicine, and pollution monitoring; examples include DNA sequencing and the tracing of interesting molecules such as those used in bioterrorism. In medicine, the feasibility of SERS to track targeted molecules *in vivo* in a mouse model was successfully demonstrated by Gambhir *et al.*[139] Since that report, numerous groups have applied targeted SERS-activated nanoparticles to track various cancer biomarkers *in vivo* in animal models.[140–144] However, the biggest limitation of SERS is the need to introduce a tag with related toxicity issues which makes this approach infeasible for human clinical applications at this time. Vo-Dinh *et al.* developed a single fiber SERS sensor that has the potential to extend SERS for *in vivo* human use without the need for a targeted particle.[145] However, no reports of *in vivo* testing of this sensor were found. Another configuration is a combination of the surface enhancement with deep Raman spectroscopy, known as SESORS. First reported by Stone *et al.*, this technique has demonstrated the potential for detecting molecule-specific SERS particles buried deeply within layers of tissues.[146,147] While this technology has not yet been implemented clinically, research for nanoparticle confinement in substrates may reduce the potential for toxicity issues.

Despite the various configurations described above, the most common configuration used in the application of Raman spectroscopy in a clinical setting is based on dispersive Raman spectroscopy in the fingerprint and/or high wavenumber region of spectrum. Spatial offset and confocal are modifications to this approach that have also been implemented and tested in a clinical setting. All the other approaches have been mostly applied to develop an improved understanding of a biological and biochemical processes rather than clinical diagnosis. Combining dispersive Raman spectroscopy with other optical (and non-optical) methods has been researched in an effort to improve performance over Raman spectroscopy alone in solving a clinical problem. Raman spectroscopy has been combined with optical coherence tomography,[148–150] optical tomography,[151] confocal reflectance

microscopy,[152,153] fluorescence and diffuse reflectance spectroscopy[154,155] to provide complementary information that can be used to further enhance the diagnostic capability of any one of these methods alone. The instrumentation considerations for making such multi-modal approaches feasible are usually challenged by the need to combine a narrow bandwidth laser and sensitive detector, essential for the very weak Raman signals with the source and detector considerations of a much brighter signal acquired using these other modalities. The resulting combinations yield a much more complicated instrument design accompanied with a higher cost device. Nevertheless, various researchers have successfully demonstrated the diagnostic advantage of these multi-modal approaches.

4. Clinical applications of Raman spectroscopy

Numerous research groups have investigated the potential of Raman spectroscopy for clinical use over the past decades and continue to find interesting medical problems for which the noted sensitivity of Raman scattering holds great promise. Various implementations of the instruments described above have been utilized in clinical studies that demonstrate the potential of Raman spectroscopy to impact medical care. In this section, we present a review of large ($n > 50$), clinical *in vivo* studies that are focused on the application of Raman spectroscopy for disease detection and sensing. These studies provide a snapshot of the current state of the field in the clinical implementation of this technique (Table 2). By far, the most common clinical target under investigation with Raman spectroscopy is cancer. Large clinical studies have seen ongoing work in several organ systems, all of which have traits in common: a need for improved early detection with high sensitivity and specificity, well-characterized disease processes, and relative ease of access to the organ under study. The specific instruments utilized in these studies differ slightly but all of the designs are driven by the anatomical target of interest. It is also of interest to note that all published studies of large clinical studies have been performed by the same few research groups pointing to the need for more research to translate the scope of Raman spectroscopy to *in vivo* human studies (Table 2).

a. Cervix

Cervical cancer is a highly preventable disease, as progression from precancer (or dysplasia) to cancer takes many years, providing a wide detection and treatment window. Developed countries have implemented vigorous screening programs that have dramatically reduced cervical cancer rates. Unfortunately, in developing nations where limited resources prevent large-scale screening, cervical cancer is one of the most common causes of cancer-related death among women comprising approximately 90% of 265 000 cervical cancer deaths worldwide.[156] Raman spectroscopy has been evaluated as an early diagnostic tool for cervical cancers and precancers over the past two decades. Our group demonstrated that Raman scattering was sensitive to normal, benign, low grade, and high grade dysplastic tissues *in vivo*.[157] By integrating analytical algorithms with data collection, diagnostic accuracies as high as 88% were achieved. Further investigation found that by incorporating hormonal/menopausal status, the predictive performance improved to 94%.[158] Continuing work has identified cervical inflammation, parity status, and body mass index as additional variables to be considered but identified limited influence of other patient variables

including race/ethnicity and socio-economic status on Raman scattering based disease discrimination.[93,159]

The well-defined nature of the disease and easy accessibility of the cervix have allowed many researchers to pursue diagnostic research in this organ *in vivo*. Several different groups have used fiber based Raman systems for diagnosis and correlated their findings with colposcopy. These have used a variety of fiber probe designs and different multivariate statistical methods to achieve a range of performance estimates as shown in Table 2.[93,157,160–163] In other cervical cancer studies, Huang *et al.* developed a simultaneous fingerprint and high-wavenumber confocal Raman system for cervical precancer detection and demonstrated the performance of this combined approach in 84 patients with sensitivity of 81% and specificity of 87%.[163] Zeng *et al.* tested the feasibility of a label free blood test based on blood plasma SERS on samples from 60 cervical cancer patients and obtained a sensitivity and specificity of 96% and 92% respectively when using multivariate diagnostic algorithms.[164] Other results have demonstrated the potential of Raman spectroscopy to differentiate between responders and non-responders to radio-therapy on biopsies from patients with cervical cancer[165] and to detect high risk strains of the human papilloma virus in cervical cells.[166] However these results need to be independently validated in a large study cohort. A recent review article on the application of Raman spectroscopy for cervical cancer presents an excellent summary of all relevant studies in a table.[167] Beyond the realm of cancer detection, our group has demonstrated the potential of Raman spectroscopy to track biochemical changes in the cervix during pregnancy and develop an understanding of cervical remodeling that occurs throughout pregnancy and parturition.[168,169]

b. Skin

As the major organ in the integumentary system, the skin is both the outer barrier of the body to the external world as well as the tissue that is easiest to interrogate with light. Melanocytic and non-melanocytic cancers have different cellular origins, but collectively comprise the most common cancers in the world.[170] As a surface organ malignancy, skin cancers are among the easiest to study with optical techniques; however, the complex, turbid nature of the skin makes it one of the most challenging clinical targets for optical diagnostics and monitoring. Early studies used Raman spectroscopy to extract water concentration profiles in human skin while demonstrating the feasibility of *in vivo* Raman spectroscopy for clinical monitoring.[171] Since then, much of skin Raman research has focused on the investigation of Raman based diagnostics. These studies also resulted in developing portable systems that were directly applicable to the clinical workflow, with instruments that can make measurements with integration times under 1 second.[6,8,56] A number of groups have invested significant effort in studying skin cancers in order to improve patient care and as a result, skin cancer studies have some of the highest recruitment of any Raman studies published, as related in Table 2.[6,154,172–174] Zeng *et al.* utilized a Raman instrument to study melanocytic and non-melanocytic as well as malignant and premalignant melanocytic lesions from 453 patients: discrimination of cancer and precancer *versus* benign lesions demonstrated a 90–99% sensitivity, with a related specificity of 15–54%.[6] This work suggests that Raman techniques can be used to reduce the need for unnecessary biopsies to a significant degree, potentially by 50–100%. Other groups have utilized multimodal

approaches, leveraging the strengths of Raman spectroscopy with a combination of fluorescence and diffuse reflectance techniques in order to improve diagnostic outcomes. In one such report of 76 patients, Raman spectroscopy alone was demonstrated to achieve 100% sensitivity and specificity for discriminating melanoma from benign pigmented lesions, but only 72% sensitivity and 64% specificity in separating non-melanoma skin cancers from precancers and 68% sensitivity and 55% specificity for distinguishing non-melanoma cancers and precancers from normal tissues. However, when combined with fluorescence and diffuse reflectance features, those same comparisons achieved 100/100%, 95/71%, and 90/85% sensitivities/specificities, respectively.[154] In other Raman skin research not related to cancer, Irvine *et al.* studied atopic dermatitis in 132 children, correlating natural moisturizing factor signals obtained *via* Raman scattering with genetic screening for filaggrin mutations common in atopic dermatitis.[175] The results of this study found that Raman signals achieved 98.7% sensitivity and 86.8% specificity in identifying atopic dermatitis associated with these mutations. Raman spectral signatures of skin carotenoids have also been investigated using a 488 nm based resonance approach to profile the intake of fruits and vegetables in preschool aged children.[115] This study demonstrated a correlation of Raman signatures with parent-reported family participation in a nutritional-education and -quality program, further demonstrating the exquisite sensitivity of Raman scattering to biochemical components.

c. Gastrointestinal tract

The gastrointestinal tract encompasses the digestive system from the mouth, through the esophagus, stomach, intestines, colon to the rectum. The entire organ system, with the exception of parts of the small intestine, is accessible directly (to the mouth) or *via* an endoscope. In developing Raman spectroscopy as a diagnostic tool for the GI tract, the challenge is in the development of a fiber probe that can be inserted through the endoscope and placed in contact with the tissue of interest in a stable manner for the duration of data acquisition. Numerous groups have focused their attention on various parts of this organ system for Raman based detection.

i. Mouth—Oral tissue is particularly easy to access since endoscopy is not required, mitigating the size constraints of the probe for *in vivo* Raman measurements. Oral cancer incidence has been increasing over the last 40 years in the US and is a larger problem globally. For example, it accounts for 10% of all cancers in India.[156] This cancer can rapidly spread, which emphasizes the need for early detection and monitoring. Murali Krishna *et al.* report the discrimination of normal control, premalignant, and cancerous sites from 104 patients with prediction accuracies ranging from 72–96%.[176] In a more recent study, the same group investigated the potential for Raman spectroscopy to detect malignancy associated changes/cancer field effects in a cohort of 84 oral cancer and age-matched control patients.[177] Comparison of non-cancer locations in a smoking and non-smoking population demonstrated prediction accuracies from 75–98% with most of the misclassifications occurring between control locations in cancer patients and locations in smoking healthy controls. This work further demonstrates the sensitivity of Raman scattering to subtle biochemical changes which may precede macroscopic disease.[178,179] Another group reported the discrimination of normal oral tissue from three separate lesion categories with

per-class accuracies ranging from 82–89% in 199 patients and 96% sensitivity and 99% specificities for normal *versus* malignant and 99% and 98% respectively, for normal *versus* potentially malignant.[180] One variability study of age and tobacco-related pathological change for oral cancer and precancer demonstrated sensitivity to age-related changes in Raman spectra, however the inclusion of this diverse control population had no impact on classification of normal and abnormal conditions.[181] Given the critical need for oral cancer detection particularly in low resource settings and the excellent performance that can be achieved in its detection with Raman spectroscopy, this area of research is ripe for clinical translation but needs a low cost instrument for its success. The optical device market has seen a recent increase in the number of handheld Raman devices available commercially; these are sold mostly for the identification of pure chemicals and trace elements. However, these devices indicate that the technology exists for the miniaturization of current clinical Raman systems which could in turn make the prospect of commercial translation of Raman systems in low resource settings a reality.

ii. Esophagus—Barrett's esophagus is a consequence of gastroesophageal reflux that has been associated with an increased risk of esophageal adenocarcinoma. By adapting Raman fiber optic probe designs for endoscopic compatibility, *in situ* measurements of this disease target have been enabled by many groups. Wilson *et al.* demonstrated the potential for *in vivo* spectral acquisition in a cohort of 65 Barrett's esophagus patients, with sensitivities and specificities of 86–88% and 88–89%, respectively for discriminating dysplastic and high-risk lesions from non-dysplastic and low-risk cases.[82] This demonstration of a clinically-useful Raman instrument with endoscopic compatibility and 5 second integration times was an early indication of the ability of *in vivo* Raman spectroscopy to access an internal organ. More recent work by another group has demonstrated real-time performance of Raman spectroscopy during endoscopy in 373 patients with integration times of 0.2 seconds per acquisition and could discriminate high-grade dysplastic Barrett's esophagus from normal and non-dysplastic tissue with 87% sensitivity and 84.7% sensitivity.[101] Other work has demonstrated the importance of considering the anatomical location of a Raman measurement; in a study of 107 patients, inter-organ variability (between the esophagus and stomach) was significant compared to intra-organ variability and neoplastic change.[99] These results support the need for comprehensive libraries of disease spectra and a thorough understanding of healthy and diseased tissues.

iii. Stomach—As a leading cause of cancer-related death worldwide,[156] stomach cancer has been another popular detection target for Raman spectroscopy.[182–184] As with the esophagus, integrating Raman fiber probes with standard endoscopes has enabled *in vivo* evaluation of gastric malignancies. Utilizing an endoscope compatible probe, linear component tissue model, and classification and regression trees, Huang *et al.* reported 94% sensitivity and 93.4% specificity for discriminating normal gastric tissue from cancer in 67 patients undergoing endoscopy with biopsy.[185] Huang *et al.* have also reported a statistically robust study where 450 patients undergoing upper endoscopy were measured with Raman spectroscopy to train a discrimination algorithm.[186] This work was one of the first reports to prospectively discriminate gastric precancer in real-time using Raman spectroscopy, achieving a sensitivity of 81% and a specificity of 88%. In another study by the same group,

researchers investigated stomach ulcers in 71 patients and found that Raman endoscopic measurements could differentiate normal mucosa, benign and malignant ulcers with 82–90% sensitivity and 93–95% specificity.[187] A related report by this group investigated the ability of Raman techniques to perform multi-class discrimination of normal, precancer, and early stage gastric cancer in a cohort of 83 patients, and demonstrated sensitivity to early stages of the carcinogenic process.[188] Finally, a report combining Raman techniques with near-infrared autofluorescence signatures ($n = 81$, 97.9% sensitivity & 91.5% specificity)[189] demonstrated similar results for *in vivo* detection for cohorts gastric cancer patients.

iv. Colon/intestine—Colorectal cancer is a major disease entity, ranking among the top three cancers worldwide for estimated new cases and cancer-related deaths.[156] Colonoscopy is the most sensitive technique available for screening and early detection of cancer or precancerous polyps and routine colonoscopy screening for adults over 50 has become the standard in countries like the United States. However, benign polyps often develop, which can limit its sensitivity and potentially complicate intervention. Preliminary Raman studies based on *ex vivo* samples and small *in vivo* cohorts have been reported, discriminating benign and malignant polyps. One *in vivo* study has investigated the impact of the colon segment on the acquired Raman signal from 50 colonoscopy patients, but found that the between-segment variability was less influential than malignant status.[190] The same group has since reported an *in vivo* study combining both fingerprint and high-wavenumber Raman spectroscopy during endoscopy in order to achieve 90% sensitivity and 83% specificity for separating adenomatous and hyperplastic polyps in real-time.[128] In other studies, our group has demonstrated the potential for endoscopic Raman spectroscopy to discriminate inflammatory bowel diseases in a 53 patient cohort, demonstrating the potential of Raman spectroscopy to detect subtle changes in tissues related to inflammatory diseases,[34] another significant clinical problem that has seen a rise in incidence in recent years.

d. Other diagnostic targets—While the majority of reports published on large clinical *in vivo* Raman studies have been focused on the above tissues, other diseases have also been studied with Raman spectroscopy. Lung cancer is one of the most common causes of cancer related death impacting millions of people annually.[156] Similar to other endoscopic studies with Raman scattering, investigation of this disease has been conducted in *ex vivo* samples with near 100% accuracy. A bronchoscope compatible Raman fiber probe has been used to study the potential of Raman spectroscopy for the detection of pre-neoplastic lesions in the bronchial tree in 26 patients.[191] However, no reports on the performance of this technique for a large cohort of lung cancers *in vivo* were found.

Surgical guidance is another area of active research for clinical Raman spectroscopy, where researchers have developed biopsy-needle compatible fiber probes to detect micro-calcifications for breast cancer diagnosis as well as SORS techniques to determine breast cancer margin status during surgical resection with excellent results. Raman spectra of core needle biopsies could successfully be used to identify the presence of micro-calcification in these specimens with 82% accuracy.[192] Depth-resolved SORS was used to assess the ability of this technique to detect the presence of cancer cells in excised breast specimens for margin assessment with 95% sensitivity and 100% specificity.[132] A large clinical study is

currently in progress to validate these findings intra-operatively. Another study has focused on the ability of Raman spectroscopy to assess axillary lymph nodes during breast surgery.[193] Preliminary reports for this study utilized frozen tissue sections of lymph nodes from 58 patients immediately after excision from the body and reported 81% sensitivity and 97% specificity. However, the authors indicate that freshly excised samples could be analyzed for intra-operative evaluation. Another application for Raman spectroscopy in surgical guidance is for brain surgery. While restricted to small cohort studies at this point, researchers have characterized a surgery compatible Raman probe based system[194] and demonstrated discrimination of normal brain from dense cancer and normal brain invaded by cancer cells with up to 93% sensitivity and 91% specificity for grade 2 to grade 4 gliomas in 17 patients.[195] This work shows continued promise for surgical guidance based on Raman scattering techniques however, it also requires expanded recruitment for validation.

A majority of the research for Raman spectroscopy techniques has focused on disease diagnosis of tissues *in situ.* However, clinically relevant diagnostics have also been investigated for samples removed from the body, especially pertaining to blood analytes. Puppels *et al.* published work utilizing a spectral library to prospectively and rapidly evaluate blood cultures for bacterial and fungal pathogens, achieving 92% classification accuracy from 121 patient samples.[196] More commonly, researchers introduce SERS particles into *ex vivo* specimens in order to improve sensitivities. These have been applied for numerous detection endpoints including a recent publication for nasopharyngeal cancer detection[197] where blood plasma samples from 156 patients were analyzed with SERS. The study demonstrated 95% sensitivity and 91% specificity for discriminating healthy volunteers from cancer patients. Liu *et al.* used SERS particles with serum from healthy and bladder cancer patients in order to improve early stage detection. By combining the sensitivity of SERS with advanced machine learning genetic algorithms, the researchers were able to achieve 94% diagnostic accuracy in a cohort of 91 patients.[198] Zeng *et al.* have likewise investigate SERS techniques for blood plasma analysis aimed at improved gastric cancer detection.[199] Samples from 65 patients were analyzed with polarized illumination of SERS particles and multivariate techniques. The study indicated great promise for specific circularly-polarization regimes with 100% sensitivity and 97% specificity for non-invasive gastric cancer detection. Another long-standing non-invasive target includes blood glucose monitoring. Feld *et al.* developed compound hyper-and parabolic concentrators for transdermal blood glucose measurements, however, there have been no large cohort studies reported with this device.[38,84] Other reports have utilized Raman scattering to look at cerebral spinal fluid samples from 61 patients *ex vivo* to diagnoses tuberculous meningitis and achieved 91% sensitivity and 82% specificity.[200] This is just a glimpse of the numerous *ex vivo* applications of Raman spectroscopic techniques that are relevant for clinical detection and diagnostics.

Raman spectroscopy has been used in the eye to study such conditions as macular degeneration. Gellerman *et al.* developed a resonance Raman approach at 488 nm to study the impact of carotenoids in the skin and eye.[113] In one application of this approach, Chakaravarthy *et al.*, measured macular pigment from 107 patients and correlated with heterochromatic flicker photometry to evaluate antioxidant pigment of the retina, however, the correlations were low and further investigation was merited.[114] Using the same

approach, Stevenson *et al.* demonstrated the improved effect of antioxidant supplementation in age related macular degeneration patients in a study of 433 patients *in vivo*.[112]

5. Summary

Despite the impressive work presented here in a selection of clinical fields, there remain a number of challenges that stand in the way of clinical translation for Raman based technologies for widespread human use. Demonstrating the safety of these devices to regulatory agencies is a vital step that must be undertaken for translation. Practically speaking, there is a need for robust system design with consistent internal calibration, such that with little training, a user can setup a system and collect repeatable data. For this to be realized, low-cost or long-lasting, durable, high-performance fiber optic probes (or an equivalent light delivery device) are required. Having reliable and consistent performance for interfacing the sample and system is pivotal for the transition from research instrument to clinical relevance. To this end, there is also a need for inter-system calibration and large libraries of spectral data that can be transferred and compared between instruments, to expand the utility of the devices for multiple medical targets. Standardized and reliable methods for data analysis are necessary to condense the feature-rich Raman spectra obtained by these instruments into not only the salient features used for a clinical evaluation, but also communicated to the user in a simple, easily interpretable format, including clinically relevant metrics for evaluation (ROC, sensitivity/specificity). Preliminary work on many of these aspects for clinical translation are ongoing, but continued effort is needed to facilitate the transition from benchtop to bedside. Of course, it is of the utmost importance that the technologies developed provide new and meaningful information about a clinical target; therefore, seeking collaboration and input from the medical community is paramount to ensure that research efforts of Raman techniques are directed at relevant needs in medicine and surgery. Finally, the largest obstacle at this point to clinical translation is the need to demonstrate the added value of these optical technologies over or in parallel with existing medical devices in large cohorts studies based on patient outcomes and relative to meaningful and accepted gold standards.

The various applications described above demonstrate the potential of Raman spectroscopy to affect patient care. And yet few systems based on Raman spectroscopy have been processed through regulatory approval and commercialized successfully. The external barriers towards the adoption of this technology lies in the limited size of the target market revenue which tends to hold back potential industrial partners and investors. Regardless, there have been some successes including the system by River Diagnostics which has successfully sold Raman instruments for the assessment of skin in the cosmetic industry (albeit not for a clinical application) and Verisante Technology which has most recently released Raman based devices for oral and skin cancer diagnosis. These commercial devices indicate that the barriers to the clinical implementation of Raman spectroscopy are not insurmountable and widespread acceptance of this technology can be achieved.

References

1. Raman C, Krishnan K. Nature. 1928; 121:501–502.

2. Ferraro, JR.; Nakamoto, K. Introductory Raman Spectroscopy. Academic Press; San Diego, CA: 1994.
3. Williams AC, Barry BW, Edwards HG, Farwell DW. Pharm Res. 1993; 10:1642–1647. [PubMed: 8290479]
4. Bergholt MS, Zheng W, Ho KY, Teh M, Yeoh KG, Yan So JB, Shabbir A, Huang Z. Gastroenterology. 2014; 146:27–32. [PubMed: 24216327]
5. Huang Z, Teh SK, Zheng W, Mo J, Lin K, Shao X, Ho KY, Teh M, Yeoh KG. Opt Lett. 2009; 34:758–760. [PubMed: 19282923]
6. Lui H, Zhao J, McLean D, Zeng H. Cancer Res. 2012; 72:2491–2500. [PubMed: 22434431]
7. Lieber CA, Mahadevan-Jansen A. Appl Spectrosc. 2003; 57:1363–1367. [PubMed: 14658149]
8. Zhao J, Lui H, McLean DI, Zeng H. Skin Res Technol. 2008; 14:484–492. [PubMed: 18937786]
9. Motz JT, Gandhi SJ, Scepanovic OR, Haka AS, Kramer JR, Dasari RR, Feld MS. J Biomed Opt. 2005; 10:031113. [PubMed: 16229638]
10. Hanlon EB, Manoharan R, Koo TW, Shafer KE, Motz JT, Fitzmaurice M, Kramer JR, Itzkan I, Dasari RR, Feld MS. Phys Med Biol. 2000; 45:R1–R59. [PubMed: 10701500]
11.
A. Standard, Inc., New York, 1993.
12. Patil CA, Pence IJ, Lieber CA, Mahadevan-Jansen A. Opt Lett. 2014; 39:303–306. [PubMed: 24562132]
13. Welch AJ. IEEE J Quantum Electron. 1984; 20:1471–1481.
14. Manoharan, R.; Wang, Y.; Boustany, NN.; Brennan, JF., III; Baraga, JJ.; Dasari, RR.; Van Dam, J.; Singer, S.; Feld, MS. Raman spectroscopy for cancer detection: instrument development and tissue diagnosis. International Symposium on Biomedical Optics Europe'94; Lille, France. 1994. p. 128-132.
15. Frank CJ, McCreery RL, Redd DC. Anal Chem. 1995; 67:777–783. [PubMed: 7762814]
16. Clarke RH, Hanlon EB, Isner JM, Brody H. Appl Opt. 1987; 26:3175–3177. [PubMed: 20490030]
17. Yu NT, East EJ. J Biol Chem. 1975; 250:2196–2202. [PubMed: 1167863]
18. Nie S, Bergbauer K, Ho J, Kuck J, Yu N. Spectroscopy. 1990; 5:24.
19. Puppels G, De Mul F, Otto C, Greve J, Robert-Nicoud M, Arndt-Jovin D, Jovin T. Nature. 1990; 347:301–303.10.1038/347301a0 [PubMed: 2205805]
20. Coldren, LA.; Corzine, SW.; Mashanovitch, ML. Diode Lasers and Photonic Integrated Circuits. Wiley; 2012.
21. Fleming MW, Mooradian A. IEEE J Quantum Electron. 1981; 17:44–59.
22. Rudder SL, Connolly JC, Steckman GJ. Proc SPIE. 2006; 61010I10.1117/12.646791
23. Wang W, Major A, Paliwal J. Appl Spectrosc Rev. 2011; 47:116–143.
24. Latka I, Dochow S, Krafft C, Dietzek B, Popp J. Laser Photonics Rev. 2013; 7:698–731.
25. Myrick M, Angel S. Appl Spectrosc. 1990; 44:565–570.
26. Utzinger U, Richards-Kortum RR. J Biomed Opt. 2003; 8:121–147. [PubMed: 12542388]
27. Myrick ML, Angel SM, Desiderio R. Appl Opt. 1990; 29:1333–1344. [PubMed: 20563003]
28. Mahadevan-Jansen A, Richards-Kortum R. J Biomed Opt. 1996; 1:31–70. [PubMed: 23014644]
29. Shim MG, Wilson BC, Marple E, Wach M. Appl Spectrosc. 1999; 53:619–627.
30. Matousek P. Appl Spectrosc. 2007; 61:845–854. [PubMed: 17716403]
31. Broeng J, Barkou SE, Sondergaard T, Bjarklev A. Opt Lett. 2000; 25:96–98. [PubMed: 18059794]
32. Broeng J, Mogilevstev D, Barkou SE, Bjarklev A. Opt Fiber Technol. 1999; 5:305–330.
33. Mahadevan-Jansen, A.; Patil, CA.; Pence, IJ. Biomedical Photonics Handbook. 2. Vo-Dinh, T., editor. CRC Press; Boca Raton, FL: 2014.
34. Pence IJ, Nguyen QT, Bi X, Herline AJ, Beaulieu DM, Horst SN, Schwartz DA, Mahadevan-Jansen A. Proc SPIE. 2014; 89390R10.1117/12.2042795
35. Mahadevan-Jansen A, Mitchell MF, Ramanujam N, Utzinger U, Richards-Kortum R. Photochem Photobiol. 1998; 68:427–431. [PubMed: 9747597]

36. Motz JT, Hunter M, Galindo L, Kramer JR, Dasari RR, Feld MS. J Biomed Opt. 2005; 10:031113. [PubMed: 16229638]
37. Schwab SD, McCreery RL. Anal Chem. 1984; 56:2199–2204.
38. Tanaka K, Pacheco MT, Brennan JF III, Itzkan I, Berger AJ, Dasari RR, Feld MS. Appl Opt. 1996; 35:758–763. [PubMed: 21069066]
39. Dochow S, Latka I, Becker M, Spittel R, Kobelke J, Schuster K, Graf A, Bruckner S, Unger S, Rothhardt M, Dietzek B, Krafft C, Popp J. Opt Express. 2012; 20:20156–20169. [PubMed: 23037068]
40. P. Instruments. Spectroscopic etaloning in back illuminated ccds. http://www.princetoninstruments.com/cms/index.php/library/51-ccd-primer/149-spectroscopic-etaloning-in-back-illuminated-ccds
41. Andor Technologies. Optical Etaloning in CCDs and EMCCDs. http://www.andor.com/pdfs/literature/Optical_Etaloning_in_CCDs_and_EMCCDs.pdf
42. Horiba Scientific. Etalon Fringe Suppression. http://www.horiba.com/fileadmin/uploads/Scientific/Documents/OSD/OSD-Etalon_Fringe_Suppression.pdf
43. Bonnier F, Ali S, Knief P, Meade AD, Hornebeck W, Lambkin H, Flynn K, McDonagh V, Healy C, Lee TC, Lyng FM, Byrne HJ. J Raman Spectrosc. 2011; 42:1711.
44. Huang ZW, Zeng HS, Hamzavi I, Alajlan A, Tan E, McLean DI, Lui H. J Biomed Opt. 2006; 11:034010.
45. Lakowicz, J. Principles of fluorescence spectroscopy. 1983.
46. P. Instruments. Introduction to Scientific InGaAs FPA cameras. 2012.
47. Kawabata T, Mizuno T, Okazaki S, Hiramatsu M, Setoguchil T, Kikuchi H, Yamamoto M, Hiramatsu Y, Kondo K, Baba M, Ohta M, Kamiya K, Tanaka T, Suzuki S, Konno H. J Gastroenterol. 2008; 43:283–290. [PubMed: 18458844]
48. Min YK, Yamamoto T, Kohda E, Ito T, Hamaguchi H. J Raman Spectrosc. 2005; 36:73–76.
49. Pence IJ, Patil CA, Lieber CA, Mahadevan-Jansen A. Biomed Opt Express. 2015; 6:2724–2737. [PubMed: 26309739]
50. Lerner JM. Cytometry, Part A. 2006; 69:712–734.
51. Battey DE, Slater JB, Wludyka R, Owen H, Pallister DM, Morris MD. Appl Spectrosc. 1993; 47:1913–1919.
52. Tedesco JM, Owen H, Pallister DM, Morris MD. Anal Chem. 1993; 65:A441–A449.
53. Kessler, TJ.; Barone, J.; Kellogg, C.; Huang, H. Holographic Transmission Gratings for Spectral Dispersion. Radha, PB., editor. Vol. 82. University of Rochester Laboratory for Laser Energetics; Springfield, VA: 2000.
54. Keltner Z, Kayima K, Lanzarotta A, Lavalle L, Canepa M, Dowrey AE, Story GM, Marcott C, Sommer AJ. Appl Spectrosc. 2007; 61:909–915. [PubMed: 17910785]
55. Lieber CA, Kanter EM, Mahadevan-Jansen A. Appl Spectrosc. 2008; 62:575–582. [PubMed: 18498700]
56. Huang Z, Zeng H, Hamzavi I, McLean DI, Lui H. Opt Lett. 2001; 26:1782–1784. [PubMed: 18059697]
57. Marcet S, Verhaegen M, Blais-Ouellette S, Martel R. Proc SPIE. 2012; 84121J10.1117/12.2000479
58. Stone N, Stavroulaki P, Kendall C, Birchall M, Barr H. Laryngoscope. 2000; 110:1756–1763. [PubMed: 11037840]
59. Utzinger U, Heintzelman DL, Mahadevan-Jansen A, Malpica A, Follen M, Richards-Kortum R. Appl Spectrosc. 2001; 55:955–959.
60. Pence IJ, Vargis E, Mahadevan-Jansen A. Appl Spectrosc. 2013; 67:789–800. [PubMed: 23816132]
61. Mahadevan-Jansen A, Richards-Kortum R. J Biomed Opt. 1996; 1:31–70. [PubMed: 23014644]
62. Choquette SJ, Etz ES, Hurst WS, Blackburn DH, Leigh SD. Appl Spectrosc. 2007; 61:117–129. [PubMed: 17331302]
63. Krishnamoorthi, H.; Mahadevan-Jansen, A. Biomedical Vibrational Spectroscopy IV. San Francisco, CA: 2010.

64. Mosier-Boss PA, Lieberman S, Newbery R. Appl Spectrosc. 1995; 49:630–638.
65. Van Duyne RP, Jeanmaire DL, Shriver D. Anal Chem. 1974; 46:213–222.
66. O'Grady A, Dennis AC, Denvir D, McGarvey JJ, Bell SE. Anal Chem. 2001; 73:2058–2065. [PubMed: 11354491]
67. Zhang D, Ben-Amotz D. Appl Spectrosc. 2000; 54:1379–1383.
68. Barclay V, Bonner R, Hamilton I. Anal Chem. 1997; 69:78–90.
69. Cai TT, Zhang D, Ben-Amotz D. Appl Spectrosc. 2001; 55:1124–1130.
70. Chen K, Zhang HY, Wei HY, Li Y. Appl Opt. 2014; 53:5559–5569. [PubMed: 25321134]
71. Vickers TJ, Wambles RE, Mann CK. Appl Spectrosc. 2001; 55:389–393.
72. Zhao J, Lui H, McLean DI, Zeng H. Appl Spectrosc. 2007; 61:1225–1232. [PubMed: 18028702]
73. Baraga JJ, Feld MS, Rava RP. Appl Spectrosc. 1992; 46:187–190.
74. De Luca AC, Mazilu M, Riches A, Herrington CS, Dholakia K. Anal Chem. 2009; 82:738–745. [PubMed: 20017474]
75. Zhang ZM, Chen S, Liang YZ. Analyst. 2010; 135:1138–1146. [PubMed: 20419267]
76. Cadusch PJ, Hlaing MM, Wade SA, McArthur SL, Stoddart PR. J Raman Spectrosc. 2013; 44:1587–1595.
77. Zhang ZM, Chen S, Liang YZ, Liu ZX, Zhang QM, Ding LX, Ye F, Zhou H. J Raman Spectrosc. 2010; 41:659–669.
78. Savitzky A, Golay MJE. Anal Chem. 1964; 36:1627–1639.
79. Edgell WF, Schmidlin E, Balk MW. Appl Spectrosc. 1980; 34:420–434.
80. Bussian BM, Hardle W. Appl Spectrosc. 1984; 38:309–313.
81. Feuerstein D, Parker KH, Boutelle MG. Anal Chem. 2009; 81:4987–4994. [PubMed: 19449858]
82. Wong Kee Song L-M, Molckovsky A, Wang KK, Burgart LJ, Dolenko B, Somorjai RL, Wilson BC. Proc SPIE. 2005; 14010.1117/12.584986
83. Ramos PM, Ruisanchez I. J Raman Spectrosc. 2005; 36:848–856.
84. Kong CR, Barman I, Dingari NC, Kang JW, Galindo L, Dasari RR, Feld MS. AIP Adv. 2011; 1:032175.
85. Liu C, Glassman WS, Zhu H, Akins D, Deckelbaum L, Stetz M, O'BRIEN K, Scott J, Alfano R. Lasers Life Sci. 1992; 4:257–264.
86. Liu CH, Das BB, Sha Glassman WL, Tang GC, Yoo KM, Zhu HR, Akins DL, Lubicz SS, Cleary J, Prudente R, et al. J Photochem Photobiol, B. 1992; 16:187–209. [PubMed: 1474426]
87. Petrich W. Appl Spectrosc Rev. 2001; 36:181–237.
88. Mahadevan-Jansen A, Mitchell MF, Ramanujam N, Malpica A, Thomsen S, Utzinger U, Richards-Kortum R. Photochem Photobiol. 1998; 68:123–132. [PubMed: 9679458]
89. Choo-Smith LP, Edwards HG, Endtz HP, Kros JM, Heule F, Barr H, Robinson JS Jr, Bruining HA, Puppels GJ. Biopolymers. 2002; 67:1–9. [PubMed: 11842408]
90. Berger AJ, Koo TW, Itzkan I, Horowitz G, Feld MS. Appl Opt. 1999; 38:2916–2926. [PubMed: 18319874]
91. Huang Z, Teh SK, Zheng W, Lin K, Ho KY, Teh M, Yeoh KG. Biosens Bioelectron. 2010; 26:383–389. [PubMed: 20729057]
92. Barman I, Dingari NC, Saha A, McGee S, Galindo LH, Liu W, Plecha D, Klein N, Dasari RR, Fitzmaurice M. Cancer Res. 2013; 73:3206–3215. [PubMed: 23729641]
93. Vargis E, Kanter EM, Majumder SK, Keller MD, Beaven RB, Rao GG, Mahadevan-Jansen A. Analyst. 2011; 136:2981–2987. [PubMed: 21666910]
94. Lednev IK, Ryzhikova E, Kazakov O, Halamkova L, Celmins D, Molho E, Zimmerman EA. Ann Neurol. 2014; 76:S94–S94.
95. Teh SK, Zheng W, Ho KY, Teh M, Yeoh KG, Huang Z. J Biomed Opt. 2008; 13:034013. [PubMed: 18601558]
96. Mahadevan-Jansen, A.; Mantsch, HH.; Puppels, GJ. Society of Photo-optical Instrumentation Engineers. Biomedical vibrational spectroscopy II; 19-20 January, 2002; San Jose, [California] USA. Bellingham, Wash: SPIE; 2002.

97. Caspers P, Lucassen G, Bruining H, Puppels G. J Raman Spectrosc. 2000; 31:813–818.
98. Shafer-Peltier KE, Haka AS, Fitzmaurice M, Crowe J, Myles J, Dasari RR, Feld MS. J Raman Spectrosc. 2002; 33:552–563.
99. Bergholt MS, Zheng W, Lin K, Ho KY, Teh M, Yeoh KG, So JBY, Huang ZW. J Biomed Opt. 2011; 16:037003. [PubMed: 21456876]
100. Huang ZW, Teh SK, Zhen W, Mo JH, Lin K, Shao XZ, Ho KY, Teh M, Yeoh KG. Opt Lett. 2009; 34:758–760. [PubMed: 19282923]
101. Bergholt MS, Zheng W, Ho KY, Teh M, Yeoh KG, So JBY, Shabbir A, Huang ZW. Gastroenterology. 2014; 146:27–32. [PubMed: 24216327]
102. Carey P. J Mol Struct. 1984; 112:337.
103. Twardowski, J.; Anzenbacher, P. Raman and IR Spectroscopy in Biology and Biochemistry. Ellis Horwood; New York: 1994.
104. Colthup, NB.; Daly, LH.; Wiberley, SE. Introduction to infrared and Raman spectroscopy. Academic Press; New York, NY: 1990.
105. Bailo E, Deckert V. Chem Soc Rev. 2008; 37:921–930. [PubMed: 18443677]
106. Masihzadeh O, Ammar DA, Kahook MY, Lei TC. Invest Ophthalmol Visual Sci. 2013; 54:3094–3101. [PubMed: 23580484]
107. Saar BG, Freudiger CW, Reichman J, Stanley CM, Holtom GR, Xie XS. Science. 2010; 330:1368–1370. [PubMed: 21127249]
108. Larsson K, Hellgren L. Experientia. 1974; 30:481–483. [PubMed: 4833665]
109. Zhou Y, Liu CH, Sun Y, Pu Y, Boydston-White S, Liu Y, Alfano RR. J Biomed Opt. 2012; 17:116021. [PubMed: 23154776]
110. Liu CH, Zhou Y, Sun Y, Li JY, Zhou LX, Boydston-White S, Masilamani V, Zhu K, Pu Y, Alfano RR. Technol Cancer Res Treat. 2013; 12:371–382. [PubMed: 23448574]
111. Byrne HJ, Baranska M, Puppels GJ, Stone N, Wood B, Gough KM, Lasch P, Heraud P, Sule-Suso J, Sockalingum GD. Analyst. 2015; 140:2066–2073. [PubMed: 25610920]
112. Beatty S, Chakravarthy U, Nolan JM, Muldrew KA, Woodside JV, Denny F, Stevenson MR. Ophthalmology. 2013; 120:600–606. [PubMed: 23218821]
113. Bernstein PS, Zhao DY, Wintch SW, Ermakov IV, McClane RW, Gellermann W. Ophthalmology. 2002; 109:1780–1787. [PubMed: 12359594]
114. Hogg RE, Anderson RS, Stevenson MR, Zlatkova MB, Chakravarthy U. Br J Ophthalmol. 2006; 91:485–490. [PubMed: 16825281]
115. Scarmo S, Henebery K, Peracchio H, Cartmel B, Lin H, Ermakov IV, Gellermann W, Bernstein PS, Duffy VB, Mayne ST. Eur J Clin Nutr. 2012; 66:555–560. [PubMed: 22434053]
116. Szymanski, HA. Raman Spectroscopy: Theory and Practice. New York: 1967.
117. Boustany NN, Manoharan R, Dasari RR, Feld MS. Appl Spectrosc. 2000; 54:24–30.
118. Asher SA. Anal Chem. 1993; 65:201A–210A.
119. Feld MS, Kramer JR. Am Heart J. 1991; 122:1803–1805. [PubMed: 1957793]
120. Klein K, Gigler AM, Aschenbrenne T, Monetti R, Bunk W, Jamitzky F, Morfill G, Stark RW, Schlegel J. Biophys J. 2012; 102:360–368. [PubMed: 22339873]
121. Kline NJ, Treado PJ. J Raman Spectrosc. 1997; 28:119–124.
122. Kirsch M, Schackert G, Salzer R, Krafft C. Anal Bioanal Chem. 2010; 398:1707–1713. [PubMed: 20734031]
123. Schulmerich MV, Cole JH, Dooley KA, Morris MD, Kreider JM, Goldstein SA, Srinivasan S, Pogue BW. J Biomed Opt. 2008; 13:020506. [PubMed: 18465948]
124. Patel II, Steuwe C, Reichelt S, Mahajan S. J Opt. 2013; 15:094006.
125. Imitola J, Cote D, Rasmussen S, Xie XS, Liu YR, Chitnis T, Sidman RL, Lin CP, Khoury SJ. J Biomed Opt. 2011; 16:021109. [PubMed: 21361672]
126. Evans CL, Xu XY, Kesari S, Xie XS, Wong STC, Young GS. Opt Express. 2007; 15:12076–12087. [PubMed: 19547572]
127. Huff TB, Cheng JX. J Microsc. 2007; 225:175–182. [PubMed: 17359252]

128. Bergholt MS, Lin K, Wang J, Zheng W, Xu H, Huang Q, Ren JL, Ho KY, Teh M, Srivastava S, Wong B, Yeoh KG, Huang Z. J Biophotonics. 2015; 9999
129. Matousek P, Clark IP, Draper ER, Morris MD, Goodship AE, Everall N, Towrie M, Finney WF, Parker AW. Appl Spectrosc. 2005; 59:393–400. [PubMed: 15901323]
130. Schulmerich MV, Finney WF, Fredricks RA, Morris MD. Appl Spectrosc. 2006; 60:109–114. [PubMed: 16542561]
131. Eliasson C, Matousek P. Anal Chem. 2007; 79:1696–1701. [PubMed: 17297975]
132. Keller M, Vargis E, Granja N, Wilson RH, Mycek MA, Kelley MC, Mahadevan-Jansen A. J Biomed Opt. 2011; 16:077006. [PubMed: 21806286]
133. Sowoidnich K, Churchwell JH, Buckley K, Kerns JG, Goodship AE, Parker AW, Matousek P. Proc SPIE. 2015; 95400910.1117/12.2183632
134. Matousek P, Draper ER, Goodship AE, Clark IP, Ronayne KL, Parker AW. Appl Spectrosc. 2006; 60:758–763. [PubMed: 16854263]
135. Cialla D, März A, Böhme R, Theil F, Weber K, Schmitt M, Popp J. Anal Bioanal Chem. 2012; 403:27–54. [PubMed: 22205182]
136. Kneipp K, Wang Y, Kneipp H, Perelman LT, Itzkan I, Dasari R, Feld MS. Phys Rev Lett. 1997; 78:1667–1670.
137. Fleischmann M, Hendra PJ, Mcquilla AJ. Chem Phys Lett. 1974; 26:163–166.
138. Jeanmaire DL, Vanduyne RP. J Electroanal Chem. 1977; 84:1–20.
139. Zavaleta CL, Smith BR, Walton I, Doering W, Davis G, Shojaei B, Natan MJ, Gambhir SS. Proc Natl Acad Sci U S A. 2009; 106:13511–13516. [PubMed: 19666578]
140. Maiti KK, Dinish US, Fu CY, Lee JJ, Soh KS, Yun SW, Bhuvaneswari R, Olivo M, Chang YT. Biosens Bioelectron. 2010; 26:398–403. [PubMed: 20801634]
141. Maiti KK, Dinish US, Samanta A, Vendrell M, Soh KS, Park SJ, Olivo M, Chang YT. Nano Today. 2012; 7:85–93.
142. Wang YL, Seebald JL, Szeto DP, Irudayaraj J. ACS Nano. 2010; 4:4039–4053. [PubMed: 20552995]
143. Dinish US, Balasundaram G, Chang YT, Olivo M. J Biophotonics. 2014; 7:956–965. [PubMed: 23963680]
144. Dinish US, Balasundaram G, Chang YT, Olivo M. Sci Rep. 2014; 4:4075. [PubMed: 24518045]
145. Stokes DL, Vo-Dinh T. Sens Actuators, B. 2000; 69:28–36.
146. Stone N, Faulds K, Graham D, Matousek P. Anal Chem. 2010; 82:3969–3973. [PubMed: 20397683]
147. Stone N, Kerssens M, Lloyd GR, Faulds K, Graham D, Matousek P. Chem Sci. 2011; 2:776–780.
148. Khan KM, Krishna H, Majumder SK, Rao KD, Gupta PK. J Biophotonics. 2014; 7:77–85. [PubMed: 23359612]
149. Patil CA, Kalkman J, Faber DJ, Nyman JS, van Leeuwen TG, Mahadevan-Jansen A. J Biomed Opt. 2011; 16:011007. [PubMed: 21280894]
150. Maher, JR.; Chuchuen, O.; Kashuba, A.; Katz, D.; Wax, A. Combined Raman Spectroscopy and Optical Coherence Tomography for Measuring Analytes in Targeted Tissues; Vancouver. 2015.
151. Desroches, J.; Goyette, A.; Pichette, J.; Jermyn, M.; Mok, K.; Mercier, J.; St-Arnaud, K.; Guiot, M-C.; Petrecca, K.; Wilson, B.; Leblond, F. Towards the combined use of Raman Spectroscopy and interstitial Optical Tomography to improve the safety and diagnostic accuracy of brain needle biopsies; Vancouver. 2015.
152. Patil CA, Arrasmith CL, Mackanos MA, Dickensheets DL, Mahadevan-Jansen A. Biomed Opt Express. 2012; 3:488–502. [PubMed: 22435097]
153. Wang H, Lee AM, Lui H, McLean DI, Zeng H. Sci Rep. 2013; 3:1890. [PubMed: 23712517]
154. Lim L, Nichols B, Migden MR, Rajaram N, Reichenberg JS, Markey MK, Ross MI, Tunnell JW. J Biomed Opt. 2014; 19:117003. [PubMed: 25375350]
155. Haka AS, Kramer JR, Dasari RR, Fitzmaurice M. J Biomed Opt. 2011; 16:011011. [PubMed: 21280898]

156. Torre LA, Bray F, Siegel RL, Ferlay J, Lortet-Tieulent J, Jemal A. Ca-Cancer J Clin. 2015; 65:87–108. [PubMed: 25651787]
157. Kanter EM, Vargis E, Majumder S, Keller MD, Woeste E, Rao GG, Mahadevan-Jansen A. J Biophotonics. 2009; 2:81–90. [PubMed: 19343687]
158. Kanter EM, Majumder S, Kanter GJ, Woeste EM, Mahadevan-Jansen A. Am J Obstet Gynecol. 2009; 200:512, e511–515. [PubMed: 19236872]
159. Vargis E, Byrd T, Logan Q, Khabele D, Mahadevan-Jansen A. J Biomed Opt. 2011; 16:117004. [PubMed: 22112136]
160. Robichaux-Viehoever A, Kanter EM, Shappell H, Billheimer D, Jones H III, Mahadevan-Jansen A. Appl Spectrosc. 2007; 61:986–993. [PubMed: 17910796]
161. Shaikh R, Dora TK, Chopra S, Maheshwari A, Kedar KD, Bharat R, Krishna CM. J Biomed Opt. 2014; 19:087001. [PubMed: 25104415]
162. Rubina S, Sathe P, Dora TK, Chopra S, Maheshwari A, Krishna CM. Proc SPIE. 2014; 89400E10.1117/12.2033937
163. Duraipandian S, Zheng W, Ng J, Low JJH, Ilancheran A, Huang ZW. J Biomed Opt. 2013; 18:067007. [PubMed: 23797897]
164. Feng S, Lin D, Lin J, Li B, Huang Z, Chen G, Zhang W, Wang L, Pan J, Chen R, Zeng H. Analyst. 2013; 138:3967–3974. [PubMed: 23529624]
165. Vidyasagar MS, Maheedhar K, Vadhiraja BM, Fernendes DJ, Kartha VB, Krishna CM. Biopolymers. 2008; 89:530–537. [PubMed: 18189303]
166. Vargis E, Tang YW, Khabele D, Mahadevan-Jansen A. Transl Oncol. 2012; 5:172–179. [PubMed: 22741036]
167. Ramos IRM, Malkin A, Lyng FM. BioMed Res Int. 2015; 2015:9.
168. Vargis E, Brown N, Williams K, Al-Hendy A, Paria BC, Reese J, Mahadevan-Jansen A. Ann Biomed Eng. 2012; 40:1814–1824. [PubMed: 22411265]
169. O'Brien CM, Vargis E, Paria BC, Bennett KA, Mahadevan-Jansen A, Reese J. Acta Paediatr. 2014; 103:715–721. [PubMed: 24628401]
170. Cancer Facts and Figures. American Cancer Society; Atlanta: 2012.
171. Caspers PJ, Lucassen GW, Carter EA, Bruining HA, Puppels GJ. J Invest Dermatol. 2001; 116:434–442. [PubMed: 11231318]
172. Schleusener J, Gluszczynska P, Reble C, Gersonde I, Helfmann J, Fluhr JW, Lademann J, Rowert-Huber J, Patzelt A, Meinke MC. Exp Dermatol. 2015; 24:767–772. [PubMed: 26010742]
173. Zakharov VP, Bratchenko IA, Myakinin OO, Artemyev DN, Khristoforova YA, Kozlov SV, Moryatov AA. Proc SPIE. 2014; 91980410.1117/12.2061667
174. Zhao J, Lui H, McLean DI, Zeng H. Conf Proc IEEE Eng Med Biol Soc. 2008; 2008:3107–3109. [PubMed: 19163364]
175. O'Regan GM, Kemperman PMJH, Sandilands A, Chen HJ, Campbell LE, Kroboth K, Watson R, Rowland M, Puppels GJ, McLean WHI, Caspers PJ, Irvine AD. J Allergy Clin Immunol. 2010; 126:574–U270. [PubMed: 20621340]
176. Singh SP, Deshmukh A, Chaturvedi P, Krishna CM. J Biomed Opt. 2012; 17:105002. [PubMed: 23223996]
177. Singh SP, Sahu A, Deshmukh A, Chaturvedi P, Krishna CM. Analyst. 2013; 138:4175–4182. [PubMed: 23392131]
178. Keller MD, Kanter EM, Mahadevan-Jansen A. Spectroscopy. 2006; 21:33–41.
179. Keller MD, Kanter EM, Lieber CA, Majumder SK, Hutchings J, Ellis DL, Beaven RB, Stone N, Mahadevan-Jansen A. Dis Markers. 2008; 25:323–337. [PubMed: 19208950]
180. Krishna H, Majumder SK, Chaturvedi P, Sidramesh M, Gupta PK. J Biophotonics. 2014; 7:690–702. [PubMed: 23821433]
181. Sahu A, Deshmukh A, Ghanate AD, Singh SP, Chaturvedi P, Krishna CM. Technol Cancer Res Treat. 2012; 11:529–541. [PubMed: 23101756]
182. Bergholt MS, Zheng W, Lin K, Ho KY, Teh M, Yeoh KG, Yan So JB, Huang Z. Int J Cancer. 2011; 128:2673–2680. [PubMed: 20726002]

183. Teh SK, Zheng W, Ho KY, Teh M, Yeoh KG, Huang Z. Br J Surg. 2010; 97:550–557. [PubMed: 20155786]
184. Wang J, Lin K, Zheng W, Ho KY, Teh M, Yeoh KG, Huang Z. Anal Bioanal Chem. 2015; 407:8303–8310. [PubMed: 25943262]
185. Huang ZW, Teh SK, Zheng W, Lin K, Ho KY, Teh M, Yeoh KG. Biosens Bioelectron. 2010; 26:383–389. [PubMed: 20729057]
186. Bergholt MS, Zheng W, Ho KY, Yeoh KG, Teh M, So JBY, Huang Z. Proc SPIE. 2014; 89390M10.1117/12.2039552
187. Bergholt MS, Zheng W, Lin K, Ho KY, Teh M, Yeoh KG, So JBY, Huang ZW. Analyst. 2010; 135:3162–3168. [PubMed: 20941419]
188. Bergholt MS, Zheng W, Ho KY, Teh M, Yeoh KG, So JB, Shabbir A, Huang Z. J Biophotonics. 2013; 6:49–59. [PubMed: 23288709]
189. Bergholt MS, Zheng W, Lin K, Ho KY, Teh M, Yeoh KG, So JB, Huang Z. Biosens Bioelectron. 2011; 26:4104–4110. [PubMed: 21550225]
190. Bergholt MS, Zheng W, Lin K, Wang J, Xu H, Ren JL, Ho KY, Teh M, Yeoh KG, Huang Z. Anal Chem. 2015; 87:960–966. [PubMed: 25495077]
191. Short MA, Lam S, McWilliams AM, Ionescu DN, Zeng HS. J Thorac Oncol. 2011; 6:1206–1214. [PubMed: 21847040]
192. Saha A, Barman I, Dingari NC, McGee S, Volynskaya Z, Galindo LH, Liu W, Plecha D, Klein N, Dasari RR, Fitzmaurice M. Biomed Opt Express. 2011; 2:2792–2803. [PubMed: 22025985]
193. Horsnell J, Stonelake P, Shetty G, Kendall C, Hutchings J, Stone N. Br J Surg. 2011; 98:26.
194. Desroches J, Jermyn M, Mok K, Lemieux-Leduc C, Mercier J, St-Arnaud K, Urmey K, Guiot MC, Marple E, Petrecca K, Leblond F. Biomed Opt Express. 2015; 6:2380–2397. [PubMed: 26203368]
195. Jermyn M, Mok K, Mercier J, Desroches J, Pichette J, Saint-Arnaud K, Bernstein L, Guiot MC, Petrecca K, Leblond F. Sci Transl Med. 2015; 7:274ra219.
196. Maquelin K, Kirschner C, Choo-Smith LP, Ngo-Thi NA, van Vreeswijk T, Stammler M, Endtz HP, Bruining HA, Naumann D, Puppels GJ. J Clin Microbiol. 2003; 41:324–329. [PubMed: 12517868]
197. Lin D, Chen GN, Feng SY, Pan JJ, Lin JQ, Huang ZF, Chen R. Appl Phys Lett. 2015; 106:013701.
198. Li S, Li L, Zeng Q, Zhang Y, Guo Z, Liu Z, Jin M, Su C, Lin L, Xu J, Liu S. Sci Rep. 2015; 5:9582. [PubMed: 25947114]
199. Feng S, Chen R, Lin J, Pan J, Wu Y, Li Y, Chen J, Zeng H. Biosens Bioelectron. 2011; 26:3167–3174. [PubMed: 21227679]
200. Sathyavathi R, Dingari NC, Barman I, Prasad PSR, Prabhakar S, Rao DN, Dasari RR, Undamatla J. J Biophotonics. 2013; 6:567–572. [PubMed: 22887773]

Biographies

Isaac Pence obtained his BE and MS degrees in biomedical engineering from Vanderbilt in 2010 and 2012, respectively. He is currently a PhD candidate in the same field at Vanderbilt. Isaac has been supported in his graduate work by a National Institutes of Health Ruth L.

Kirschstein National Research Service Award Predoctoral Fellowship. His expertise is in clinical Raman spectroscopy and the development of statistical methods for Raman data analysis. His current research is on the application of Raman spectroscopy for clinical detection of diseases in the skin and colon.

Dr Mahadevan-Jansen's primary research is the clinical translation of optical spectroscopies and imaging for disease diagnosis and guidance of therapy. She received her BSc and Msc in Physics from the University of Bombay, India, and her MS and PhD degrees in Biomedical Engineering from the University of Texas at Austin. She joined the Vanderbilt engineering faculty in 1996. She is the founding Director of the Vanderbilt Biophotonics Center and is Orrin H. Ingram Professor of Biomedical Engineering and Professor of Neurological Surgery at Vanderbilt University. Dr Mahadevan-Jansen is an associate editor of Neurophotonics as well as Applied Spectroscopy and serves as a reviewer of more than 20 journals and as chair of numerous professional conferences. She has authored over 75 peer-reviewed publications and is a fellow of the American Institute of Medical and Biological Engineering (AIMBE), and the International Society for Optical Engineering (SPIE).

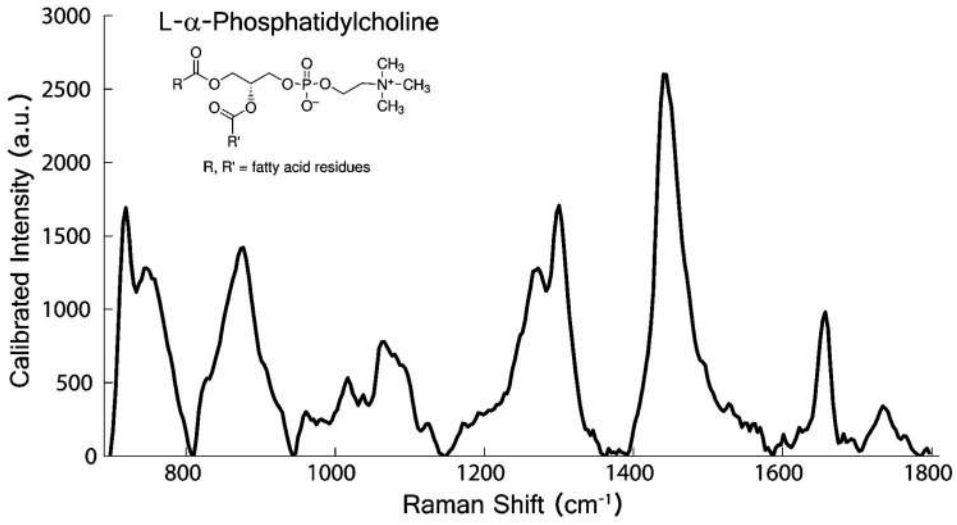

Fig. 1.

Raman spectrum of phosphatidylcholine, a phospholipid known to be present in cells and tissues, measured using a fiber optic probe based Raman system at 785 nm excitation. Characteristic spectral peaks correspond to molecular vibrations of the molecule of interest.

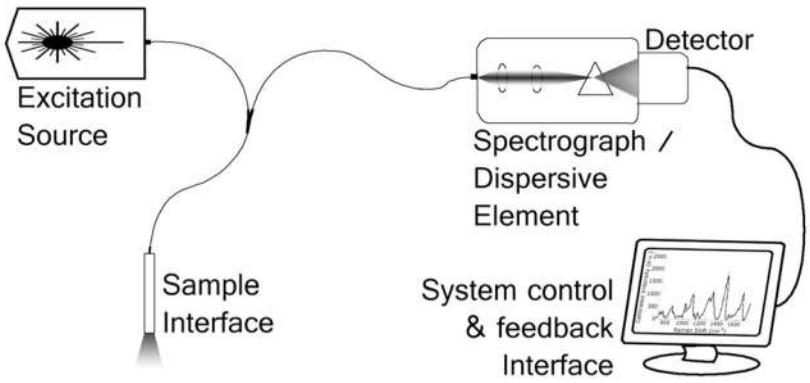

Fig. 2.
Basic schematic of an optical (including Raman) spectroscopic system.

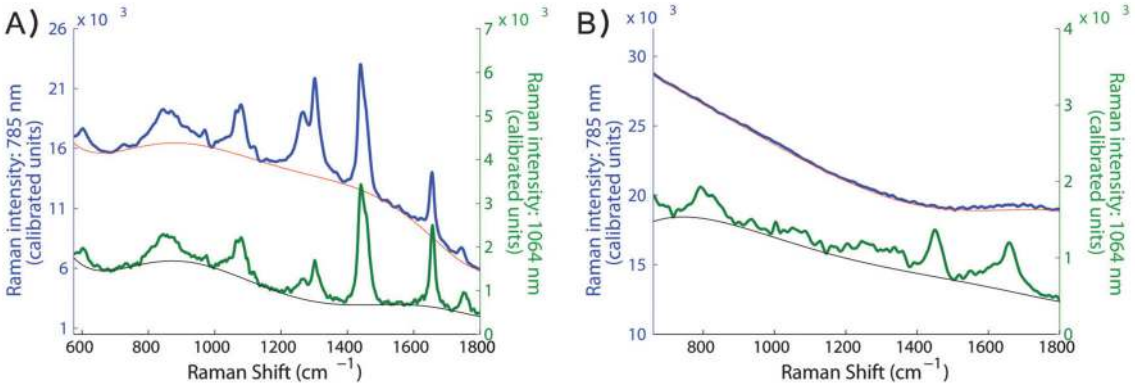

Fig. 3.

Raman scattering and autofluorescence polynomial fit signals for (A) breast and (B) kidney tissues measured *ex vivo* at 785 nm (blue) and 1064 nm (green) excitation wavelengths. Strong Raman features of breast tissue are apparent despite tissue background while low Raman intensities of the kidney are completely overwhelmed by the strong intrinsic signal at 785 nm but more readily visible at 1064 nm.

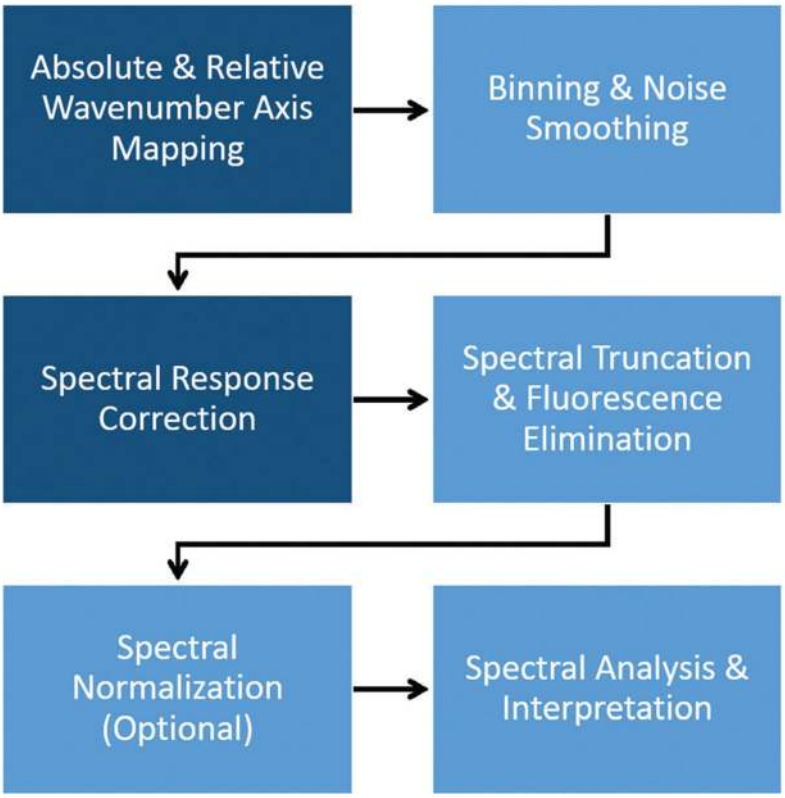

Fig. 4.

Flowchart for typical system calibration and signal processing procedures for clinical Raman spectroscopy systems. The darker shaded boxes indicate steps that require collection of reference spectra prior to data acquisition while the other steps can be implemented in-line per spectrum for system automation.

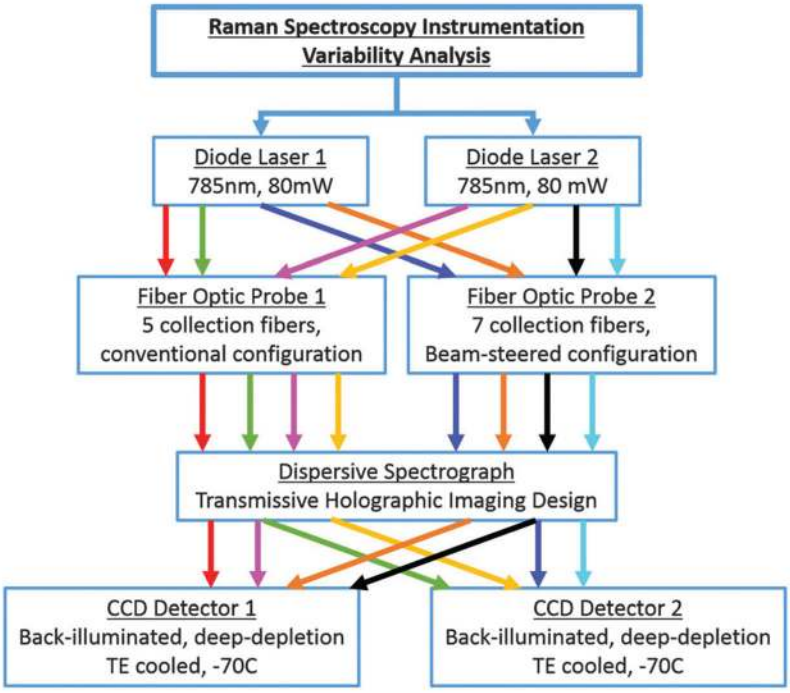

Fig. 5.

Diagram for a comparison study of clinical Raman spectroscopy system components. By varying combinations of instruments, variability studies have investigated the impact of unique components on the acquired spectral signatures. Results show that the collection leg of the system and the design of the fiber probe have the most significant contribution to the instrument variance observed in the spectra.

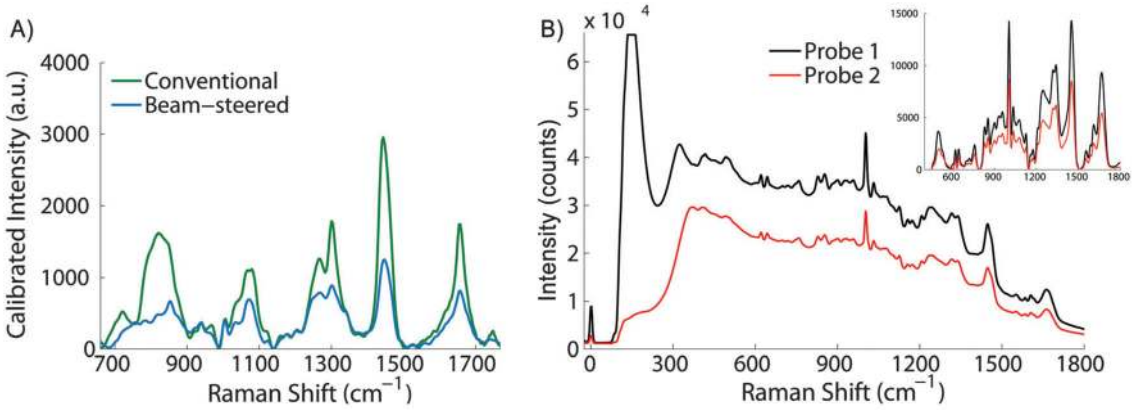

Fig. 6.

Representative Raman spectral differences that can be obtained from a single sample acquired using two different probes. (A) A conventional filtered Raman probe (green) and a beam-steered Raman probe (blue) on skin *in vivo* demonstrate unique lineshapes. (B) Two iterations of the same probe design used to measure an albumin sample demonstrate the effect of slightly different inline filters on the raw and resulting processed (inset) Raman spectrum.

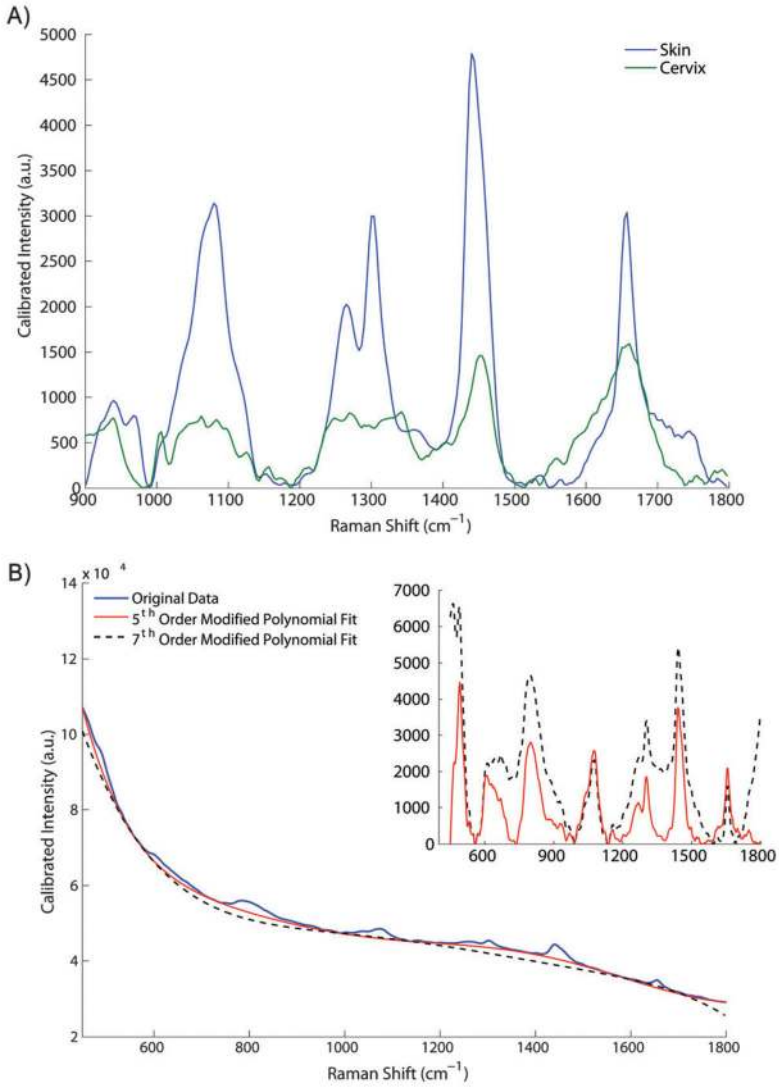

Fig. 7.

Impact of background elimination varies based on the sample or tissue measured. Fluorescence subtraction using (A) 5th order polynomial in skin and cervix yield unique shapes due to compositional differences. (B) Using a 5th *versus* 7th order polynomial in colon (processed spectra inset) demonstrates that a single polynomial fitting order may not be appropriate for all samples; higher order polynomials are used to simulate background fluorescence and subtracted to enhance the underlying Raman signal from the sample.

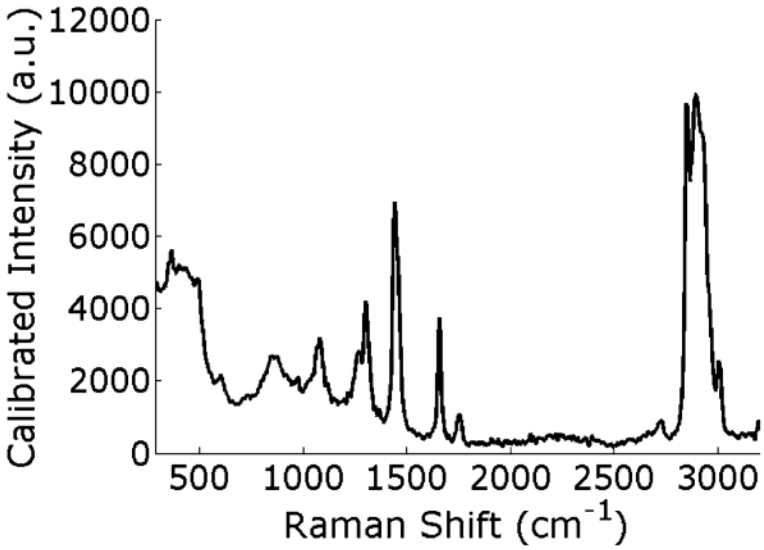

Fig. 8.

Fingerprint and high-wavenumber Raman spectrum of *ex vivo* breast tissue depicts the broad, strong features characteristic of lipid components in the tissue. Both segments of the Raman spectrum can provide valuable information for evaluation of complex sample composition.

Table 1

Summary of typical components used to build a clinically useable portable dispersive Raman system

Laser	Fiber probe	Spectrograph	CCD
B&W Tek	Visionex[a]	Kaiser f/1.8i, f/2, 2i	Princeton Instruments BRDD[b]
Sacher Lasertechnik	InPhotonics	Andor Technology Shamrock SR-303i	Andor Technology BRDD[b]
Process Instruments	Emvision	Princeton Instruments LS 785	Horiba Synapse
SDL	In-house	Horiba Labram, HE-785	Kodak KAF 1001E
Innovative Photonics Solutions		Ocean Optics QE65000	Ocean Optics QE65000

[a]These companies do not exist anymore.

[b]Back-reflected deep depletion (BRDD) CCD chip technology.

Table 2

Overview of large clinical studies ($n > 50$) performed with Raman spectroscopy *in vivo* in humans

Disease type	Raman method	Group	Publication year	Patient number	Sensitivity (%)	Specificity (%)	Ref.
Barrett's esophagus	Probe Raman	Wilson *et al.*	2005	65	86 (dysplastic), 88 (high grade)	88 (non2splastic), 89 (non-high grade)	82
Barrett's esophagus	Confocal Raman	Huang *et al.*	2014	373	87 (high grade)	84.7	101
Cervical cancer	Probe Raman	Murali Krishna *et al.*	2014	63	100	96.7	162
Cervical cancer	Probe Raman	Murali Krishna *et al.*	2014	93	100	93	161
Cervical precancer	Probe Raman	Mahadevan-Jansen *et al.*	2009	145	96.2 (premenopausal dysplasia)	90.7 (premenopausal)	157
Cervical precancer	Probe Raman	Mahadevan-Jansen *et al.*	2011	172	96.5 (dysplasia)	97.8	93
Cervical precancer	Confocal Raman	Huang *et al.*	2013	84	81 (dysplasia)	87.1	163
Cervical precancer	Probe Raman	Mahadevan-Jansen *et al.*	2007	79	89 (high grade)	81 (benign)	160
Colon cancer	Probe Raman (HF)	Huang *et al.*	2015	50	90.9 (adenoma)	83.3 (hyperplastic polyps)	128
GI cancer	Probe Raman	Huang *et al.*	2011	107	92.6 (gastric) and 90.9 (esophagus)	88.6 (gastric) and 93.9 (esophagus)	99
GI cancer	Probe Raman	Huang *et al.*	2011	81	97.9 (gastric)	91.5	189
GI cancer	Probe Raman (HF)	Huang *et al.*	2015	164	92.5 (bevelled probe) 85.8 (volumetric probe)	93.1 (bevelled probe) 88.6 (volumetric probe)	184
GI cancer	Probe Raman	Huang *et al.*	2013	83	83.3 (dysplasia) 84.9 (adenocarcinoma)	95.8 95.6	188
GI cancer	Probe Raman	Huang *et al.*	2010	67	94 (gastric)	93.4	185
GI cancer	Probe Raman	Huang *et al.*	2011	67	94.6 (gastric) 89.3 (independent validation)	94.6 97.8	182
GI cancer	Probe Raman	Huang *et al.*	2010	62	76.7 (overall)	91.4 (overall)	183
GI cancer	Probe Raman	Huang *et al.*	2014	450	81.3 (prospective)	88.3	186
GI ulcers	Probe Raman	Huang *et al.*	2010	71	82.1 (malignant ulcers) 84.7 (benign ulcers)	90.8	187
Oral cancer	Probe Raman	Murali Krishna *et al.*	2012	104	86 (tumors) 72 (pre-malignant)	74	176
Oral cancer	Probe Raman	Gupta *et al.*	2014	199	96 (malignant) 88 (premalignant), 84 (malignant) (multiclass)	99 (normal) 77 (multiclass)	180
Oral cancer	Probe Raman	Murali Krishna *et al.*	2013	84	92.7 (tumor)	98.7 (healthy control) 84 (contralateral normal)	177
Skin cancer	Probe Raman + fluorescence	Tunnell *et al.*	2014	76	100 (malignant melanoma) 90 (non-melanoma cancer)	100 (pigmented lesion) 85 (normal)	154

Disease type	Raman method	Group	Publication year	Patient number	Sensitivity (%)	Specificity (%)	Ref.
Skin cancer	Probe Raman + fluorescence	Moryatov *et al.*	2014	50	89 (malignant melanoma)	87	173
Skin cancer	Probe Raman	Meinke *et al.*	2015	104	74 (basal + squamous cell)	82	172
Skin cancer	Probe Raman	Zeng *et al.*	2012	453	90 (cancer *vs.* benign)	64	6
Skin cancer	Probe Raman	Zeng *et al.*	2008	289	91 (cancer) 97 (malignant melanoma)	75 (benign) 78 (pigmented lesion)	174
Dermatitis	Raman microscopy	Irvine *et al.*	2010	132	98.7	86.9	175
Skin carotenoids	Resonance Raman	Mayne *et al.*	2012	381			115
Macular pigment	Resonance Raman	Stevenson *et al.*	2006	97			114
Macular degeneration	Resonance Raman	Stevenson *et al.*	2013	433			112
Macular degeneration	Resonance Raman	Gellerman *et al.*	2002	201			113